# Estimating the risk of elk-to-livestock brucellosis transmission in Montana

**Authors**

Nathaniel D. Rayl[a*], Kelly M. Proffitt[b], Emily S. Almberg[b], Jennifer D. Jones[b], Jerod A. Merkle[c], Justin A. Gude[d], Paul C. Cross[a]

[a]U.S. Geological Survey, Northern Rocky Mountain Science Center, Bozeman, MT 59715, USA

[b]Montana Fish, Wildlife and Parks, Bozeman, Montana 59715, USA

[c]Wyoming Cooperative Fish and Wildlife Research Unit, Department of Zoology and Physiology, University of Wyoming, Laramie, WY 82071, USA

[d]Montana Fish, Wildlife and Parks, Helena, Montana 59720, USA

September 2018

**Executive Summary**

Wildlife reservoirs of infectious disease are a major source of human-wildlife conflict because of the risk of potential spillover associated with commingling of wildlife and livestock. In Montana, the presence of brucellosis (*Brucella abortus*) in free-ranging elk (*Cervus canadensis*) populations is of significant management concern because of the risk of disease transmission from elk to livestock. To help mitigate potential conflict, we identified how spillover risk changes through space and time using a combination of elk population, disease,

and movement data. We developed resource selection functions using telemetry data from 223 female elk to predict the relative probability of female elk occurrence on a daily basis during the 15 February-30 June transmission risk period. We combined these spatiotemporal predictions with elk seroprevalence, demography, and abortion timing data to identify when and where abortions (the primary transmission route of brucellosis) were most likely to occur. Additionally, we integrated these predictions with spatiotemporal data on livestock distribution to estimate the daily risk of livestock encountering brucellosis-induced elk abortions. We estimated that a minimum of ~17,500 adult female elk lived within our study area, which resulted in a conservative estimate of ~525 brucellosis-induced abortions each year. We predicted that approximately half of the transmission events occurred on livestock properties and 98% of those properties were private ranchlands as opposed to state or federal grazing allotments. Our fine-resolution (250-m spatial, 1-day temporal), large-scale (17,732 $km^2$) predictions of potential elk-to-livestock transmission risk provide wildlife and livestock managers with a useful tool to identify higher risk areas in space and time and proactively focus actions in these areas to separate elk and livestock to reduce spillover risk.

**Background**

The ability to predict potential areas of human-wildlife conflict remains a persistent challenge in wildlife management and conservation (Sitati et al. 2003, Woodroffe et al. 2005). Wildlife reservoirs of infectious diseases are a major source of human-wildlife conflict throughout the world (Conover 2001). These wildlife reservoirs have the potential to adversely affect the health of humans and domestic animals (Daszak et al. 2000), to negatively impact economic development and activity (Nishi et al. 2006, National Academies of Sciences, Engineering, and Medicine 2017), and to erode public support for wildlife and conservation efforts (Madden 2004, Haggerty et al. 2018). Despite these threats, there have been relatively few studies that have investigated the spatiotemporal dynamics of infectious diseases at the wildlife-livestock interface (White et al. 2017).

Epidemiological models have typically focused on the temporal components of disease transmission (Diekmann et al. 2012), while disregarding the impact of host movements on host-pathogen dynamics (Dougherty et al. 2018). This simplification of the contact process ignores host behavior, thereby disregarding an essential component of disease transmission dynamics (Zidon et al. 2017, Dougherty et al. 2018). The burgeoning field of movement ecology (Kays et al. 2015) offers useful tools to help describe and predict heterogeneous disease transmission between hosts, and to pose novel questions about the effects of animal movements on disease dynamics (Dougherty et al. 2018). For diseases with highly mobile wildlife hosts and long periods of potential transmission, integrating spatial heterogeneity of host movements into disease models may be particularly important to adequately forecast spillover dynamics (Kilpatrick et al. 2009, White et al. 2017, Merkle et al. 2018). It remains rare and challenging, however, to simultaneously model movement and epidemiological processes, because of the difficulties associated with synthesizing movement and disease ecology data streams collected at varying spatial and temporal resolutions and scales (Dougherty et al. 2018). Further complexity frequently arises because of the large amounts of data required for, and the high computational demand associated with, integrated modeling approaches (Dougherty et al. 2018).

Bovine brucellosis, caused by the bacterium *Brucella abortus*, is an important zoonotic disease worldwide, which causes chronic infections in wildlife, livestock, and humans (Pappas et al. 2006). Following an extensive eradication program by the U.S. Department of Agriculture in

the last century, brucellosis was nearly eliminated from the United States (Ragan 2002). It still persists, however, in elk (*Cervus canadensis*) and bison (*Bison bison*) populations in the Greater Yellowstone Ecosystem (GYE; National Academies of Sciences, Engineering, and Medicine 2017). Brucellosis causes reproductive failures in elk, bison, and cattle (*Bos taurus*), with transmission occurring when individuals physically contact *Brucella abortus* bacteria in aborted fetuses, placentas, or birthing fluids (Cheville et al. 1998). In the GYE, elk are the source of recent livestock infections (Rhyan et al. 2013, Kamath et al. 2016). Although rare, these spillover events are occurring with increasing frequency (Cross et al. 2013, Brennan et al. 2017), and are of substantial concern for livestock producers because of the associated costs of livestock quarantine and trade restrictions (National Academies of Sciences, Engineering, and Medicine 2017). Brucellosis appears to be spreading into new elk populations in the GYE, and the seroprevalence is increasing in some elk herds (Brennan et al. 2017, National Academies of Sciences, Engineering 2017). Currently, a designated surveillance area (DSA), within which domestic bison and cattle (hereafter, 'livestock') must be tested prior to moving to other regions, keeps the rest of the U.S. livestock population free of the disease.

Elk-to-livestock brucellosis transmission risk is complex. It involves interactions among seroprevalence, demography and density, distribution, the timing of abortions in elk, and the distribution and density of livestock (National Academies of Sciences, Engineering, and Medicine 2017). These dynamic interactions occur over relatively long time-scales and large geographic areas. The transmission period for brucellosis in elk spans more than 4 months (Cross et al. 2015). During this time, elk in the GYE migrate 10s to 100s of kilometers from winter to summer range (White et al. 2010).

Previously, Proffitt et al. (2011) developed predictive models of elk space use to estimate the risk of elk and livestock commingling during the brucellosis transmission risk period within a portion of the Montana designated brucellosis surveillance area (DSA). Since that research was conducted, the Montana Department of Fish, Wildlife and Parks initiated a multi-year brucellosis surveillance project to collect additional seroprevalence and elk movement data throughout the Montana DSA. Additionally, the seasonal timing of elk abortion events in the GYE (hereafter, "abortion phenology") was quantified for the first time (Cross et al. 2015). With these new sources of information, it is now possible to develop an integrated model that provides a more comprehensive evaluation of elk-to-livestock brucellosis transmission risk throughout the Montana DSA. Here, we combine elk seroprevalence, elk demography and density, elk distribution, elk abortion phenology, and livestock distribution data to 1) quantify the number and distribution of elk abortion events, and 2) determine the spatiotemporal overlap of elk abortion events with areas of potential livestock presence. In doing so, we provide a powerful tool to identify and proactively manage brucellosis spillover risk, and a modeling framework that can be applied to disease spillover situations worldwide.

## Methods

### *Study area*

We studied elk in the Montana DSA in southwest Montana, USA (Fig. 1A). Using elk trend counts, we estimated that there were a minimum of ~26,800 elk (and ~17,500 adult female elk) living within the DSA in 2016. The DSA is a mixture of private, Bureau of Land Management (BLM), U.S. Fish and Wildlife Service (USFWS), U.S. Forest Service (USFS), and state government lands. It is characterized by open sage-grassland communities (*Artemisia* spp., *Festuca idahoensis, Pseudoroegneria spicatum*) at lower elevations. At mid elevations, Douglas

fir (*Pseudotsuga menziesii*), and lodgepole pine (*Pinus contorta*) forests and herbaceous meadows predominate. Spruce (*Picea engelmannii*) and subalpine fir (*Abies lasiocarpa*) forests and herbaceous meadows dominate at higher elevations. Eighteen state-of-Montana elk hunting districts occur partially or entirely within the DSA, which is 17,732 $km^2$ (Fig. 1A), and has expanded several times as elk outside the boundaries have tested positive for exposure to *B. abortus*.

*Elk collaring and monitoring*

We captured adult female elk ≥2 years of age from 8 herds within the DSA by helicopter net-gunning or chemical immobilization during January-March 2005-2015 (Fig. 1B). We radio-collared elk with Global Positioning System (GPS) collars that attempted to acquire a location every 0.5, 1, or 2 h (GPS 3300L, Lotek Wireless Inc., New Market, Ontario, Canada). We monitored individual elk for 1-5 years and used pregnancy-specific protein B (PSPB) analysis (BioTracking, Moscow, Idaho, USA) to determine pregnancy. We followed Montana Department of Fish, Wildlife and Parks biomedical protocols for free-ranging Cervidae in Montana during capture and handling procedures. Most brucellosis-induced abortions in elk occur between 15 February and 30 June (Cross et al. 2015). We limited our analyses to this time period (hereafter, "risk period"). Within the risk period, we defined winter (15 February-31 March; elk on winter range), spring (1 April-31 May; elk migrating to summer range), and summer (1 June-30 June; elk on summer range) seasons based upon elk movement and aggregation patterns. Our risk period dataset consisted of 223 elk monitored from February 2005-June 2015 (280 elk-years, 1,475,613 locations).

*Evaluating commingling risk*

To predict the risk of brucellosis transmission from elk to livestock within the DSA we followed a similar framework to Merkle et al. (2018). We 1) estimated the occurrence of adult female elk using resource selection functions (RSFs; Manly et al. 2002), 2) combined our RSF elk occurrence estimates with estimates of adult female elk abundance, seroprevalence, pregnancy rates, and brucellosis-induced abortion phenology to predict the daily distribution of abortions, and 3) estimated the number of brucellosis-induced abortions occurring on public and private lands and within private ranchland and federal and state livestock allotments during an average snowfall year (Fig. 2). Our approach differed from that of Merkle's et al. (2018), by accounting for the potential distribution of livestock. In addition, to predict elk distribution, we used RSFs rather than converting parameterized step-selection functions into integro-difference equations of space use (Potts et al. 2014, Merkle et al. 2017, 2018), because we found that the RSFs performed better for these populations.

*Resource selection function development*

We developed RSFs to characterize the spatiotemporal relationship between the relative probability of female elk occurrence and landscape attributes. Because all of the Montana DSA was potential elk range, and our primary objective was to identify fine-scale spatiotemporal overlap of elk abortion events with areas of potential livestock presence, we used 3rd order RSFs (selection of patches within individual home ranges; [Meyer and Thuiller 2006]) to characterize habitat selection. Because we anticipated resource selection to vary seasonally, we built a separate RSF for each season. In our RSFs, we compared the habitat characteristics of observed locations with an equal number of available locations using a generalized linear mixed model (GLMM) with a binomial distribution, logit link, and individual-year nested within herd as the

random intercept (Gillies et al. 2006). We generated available locations by randomly sampling within a 99% contour of a bivariate normal kernel calculated with the reference bandwidth for each elk-year in each season. We assigned available locations to a specific day randomly drawn with replacement from the distribution of days of the corresponding elk-year-season observed locations. In each season our RSFs took the form:

$$w(x) = \exp(\beta_1 x_{1ijh} + \beta_2 x_{2ijh} + \cdots + \beta_u x_{uijh} + \cdots + \gamma_{0j} + \gamma_{0h}) \quad (1)$$

where $w(x)$ represented the RSF scores, $\beta_u$ was the selection coefficient for explanatory variable $x_u$ for the $i$th observation, $j$th individual-year, and $h$th herd, $\gamma_{0j}$ was the random intercept for the $j$th individual-year, and $\gamma_{0h}$ was the random intercept for the $h$th herd.

We used variables which have been shown to be important predictors of elk occurrence in our RSFs (Proffitt et al. 2011, Merkle et al. 2018). We included a suite of topographic variables (elevation, slope, terrain position index [calculated as the difference between the elevation of a cell and the mean elevation of its nearest 80 surrounding cells], and solar radiation during the risk period; 30-m resolution, U.S. Geological Survey National Elevation Dataset), distance to motorized roads (30-m resolution, U.S. Department of Commerce, Bureau of the Census), landcover type (consolidated into 4 categories: forest, shrub, agriculture, grass [reference category]; 30-m resolution, 2011 National Land Cover Database), snow cover (500-m spatial and 8-day temporal resolution, MODIS data [Hall et al. 2002]), overall productivity or biomass of a habitat patch each year calculated as the annual integrated Normalized Difference Vegetation Index (NDVI, 250-m resolution, MODIS data [Pettorelli et al. 2005]), and the phenological stage of a habitat patch calculated as the daily NDVI value (scaled between 0 and 1) of a patch (250-m resolution, calculated following the cleaning and smoothing methods of Bischof et al. [2012] and Merkle et al. [2016]).

Before building seasonal RSFs, we conducted preliminary analyses to select functional forms of continuous variables. We tested whether a linear or quadratic functional form for elevation, slope, solar radiation, and phenological stage and whether a linear or pseudothreshold (natural logarithm transformed distance + 1; Prokopenko et al. 2017) functional form for distance to motorized roads was better supported. For the functional forms of each variable in each season, we built GLMMs and determined the form with the most support using Akaike Information Criterion for small sample sizes (AICc; Burnham and Anderson 2002). We similarly evaluated support for different spatial scales for all non-time-varying variables, except distance to motorized roads (Laforge et al. 2015). For each of these variables, we iteratively calculated moving window averages (at the resolution of the original data) within concentric radii (30, 100, 250, 500, 750, 1,000 m; Ranglack et al. 2017) larger than the resolution of the original data (see Appendix S1: Table S1 in Supporting Information). We selected the spatial scale with the most support for each variable in each season by building GLMMs and determining support using AICc. We tested for collinearity between pairs of covariates prior to building seasonal RSFs and detected no issues (Pearson's correlation coefficient < 0.7 for all variables). We also evaluated our RSFs for multicollinearity using the variance inflation factor (VIF; without quadratic terms; Graham 2003), and detected no issues (VIFs for all variables ≤ 3.04; Dormann et al. 2013). To obtain maximum-likelihood estimates for GLMMs, we used adaptive Gauss-Hermite approximation with 5 integration points (Bolker et al. 2009).

We used cross-validation procedures to assess both the internal accuracy and external applicability of our RSF models. To evaluate the internal accuracy of each seasonal RSF, we used 100 repetitions of 5-fold cross validation with 10 bins of equal size, calculating the average Spearman rank correlation ($r_s$) between the withheld data and the ranked bins (Boyce et al.

2002). To assess external applicability, thereby estimating the generalizability of our space-use predictions to unsampled elk herds within the DSA, we iteratively fit seasonal RSFs using data from 7 of 8 sampled herds (3 seasons × 8 herds = 24 partial RSF models). For each partial RSF model, we reclassified the available locations of the excluded herd into 10 ordinal bins based on the percentile range of the partial RSF-predicted scores for those locations. We then calculated the $r_s$ between the frequency of occurrence of RSF-predicted scores for used locations from the excluded herd and the ranked RSF-availability bins. This allowed us to evaluate the ability of the partial RSF model to predict the space use of the excluded herd.

*Predicting brucellosis transmission risk*

We quantified the number and distribution of elk abortion events, and determined the spatiotemporal overlap of elk abortions with areas of potential livestock presence for an average snowfall year (2013) during our study period (see Appendix S2). Resource selection functions produce relative probability values that are proportional to the probability of use (Manly et al. 2002). Therefore, we estimated the predicted probability of adult female elk use $u(x, t)$ per 250 m pixel $x$, per time step $t$ (in days) within each hunting district, as:

$$u(x,t) = \frac{w_{xt}}{\sum_{i=1}^{n} w_{xt}} \quad (2)$$

where $i$ = refers to pixels 1 through $n$ for time step $t$, and $w_{xt}$ is the daily predicted RSF value of the relative probability of use by elk for a 250-m pixel $x$. The denominator served as a normalizing constant, ensuring that $\sum_{i=1}^{n} u\,(x,t)$ equaled 1. Following Merkle et al. (2018), we then calculated the predicted number of abortion events $\alpha_{xt}$ per 250 m pixel $x$, per time step $t$ (in days), as:

$$\alpha_{xt} = u(x,t) \times N_{dt} \times S_d \times y \times p_t \quad (3)$$

where $u(x, t)$ is the daily predicted probability of elk use for pixel $x$ within hunting district $d$, and $N_{dt}$ is the daily estimated number of female elk in that hunting district $d$ during time step $t$, $S_d$ is the average brucellosis seroprevalence estimated for each hunting district $d$ (Fig. 2; see Appendix S3), $y$ is a mean pregnancy rate of 90%, and $p_t$ is the predicted daily probability of aborting given an individual is seropositive and pregnant during time step $t$ (empirically estimated from Cross et al. 2015). We used a combination of samples from hunter-harvested and research-captured adult female elk to estimate herd seroprevalence (see Montana Fish, Wildlife and Parks [2015a] for details on how serostatus was determined). We distributed the estimated number of adult female elk from our sampled herds among the hunting districts of the DSA according to the movement patterns of collared females (see Appendix S3). Because we lacked movement data for some elk herds within the Montana DSA, we assumed that these unsampled herds remained within the hunting district where they were counted during winter surveys. We estimated the predicted number of abortion events $\alpha_{xt}$ per 250 m pixel $x$, per time step $t$ for each hunting district separately, and then summed all hunting districts in time step $t$ to predict abortions across the DSA. We merged hunting district 301 and hunting district 309 into one district (i.e., hunting district 301/309) because these districts were treated as one unit during winter surveys.

We combined $\alpha_{xt}$ estimates with landownership data to calculate the daily, cumulative, per-capita daily, and per-capita cumulative number of abortion events occurring on private, BLM, USFWS, USFS, and state government lands during the risk period. We did not consider the distribution of livestock within the Montana DSA in these calculations. We then calculated these same abortion metrics for areas with potential livestock grazing (cattle or domestic bison) to quantify risky areas for elk-to-livestock transmission risk on the landscape. We defined areas

of potential livestock grazing as private ranchlands in Montana with ≥0.4 hectares of grazing area (http://svc.mt.gov/msl/mtcadastral/; Proffitt et al. 2011), and federal (USFS, BLM), and state (Wildlife Management Area) grazing allotments in Montana when livestock were potentially present on the allotments during the risk period (see Appendix S4). We used turnout dates from BLM and USFS grazing records from 2014 (Wells 2017) and state grazing records from 2017 to determine when livestock were present on federal and state allotments. When abortion events occurred on allotments during time periods when livestock were not present, it did not contribute to our estimates of abortion events on that grazing type.

*Assessing uncertainty in brucellosis transmission risk*

Ideally, when combining multiple datasets to make spatiotemporal estimates of transmission risk, one would propagate the sampling errors associated with each underlying parameter. In our case, this is challenging because in some instances we had no formal assessment of sampling error or the necessary data to conduct such an assessment (e.g., elk trend count data). Additionally, we did not evaluate the influence of uncertainty in estimates of $u(x, t)$ on risk because of computational limitations associated with deriving error estimates for $u(x, t)$ on a cell-by-cell basis. Therefore, we highlight some of the uncertainties of the individual data streams below, but leave the full propagation of errors as an issue for further research.

We used elk trend count and age ratio data collected by Montana Fish, Wildlife and Parks to estimate $N_{dt}$ (see Appendix S3). These data provided a minimum estimate of the number of adult female elk, but were not corrected for visibility bias (Samuel et al. 1987). During aerial surveys in habitats similar to those encountered in our study area, detection estimates for elk have been estimated to range from as low as 64% (Jarding 2010) to as high as 95% (Anderson et al. 1998). To assess uncertainty associated with visibility bias, we calculated the number of abortion events that would have occurred within the DSA during the risk period if we had detected 64% or 95% of elk during our surveys. To investigate uncertainty associated with annual abortion rates, we estimated the number of abortion events within the DSA during the risk period using 95% confidence interval estimates for the proportion of seropositive and pregnant female elk that abort (Cross et al. 2015; 95% CI proportion aborting = 0.11, 0.23).

We randomly generated 1,000 seroprevalence estimates for each hunting district to evaluate uncertainty associated with brucellosis seroprevalence data. We used independent Bernoulli trials to generate seroprevalence estimates for hunting districts with data collected during the multi-year brucellosis surveillance project (see Appendix S3). For hunting districts without seroprevalence data from this project, we used 1,000 random draws from the predictive posterior distributions of seroprevalence in 2014 from Brennan et al. (2017). For each seroprevalence estimate, we calculated the number of abortion events within the DSA during the risk period, and report the 95% range of these abortion events. We conducted all analyses in program R version 3.3.1 (R Development Core Team 2016), using lme4 to fit GLMMs.

**Results**

In our preliminary analyses of resource selection, we found stronger support in all seasons for quadratic functional forms for elevation, slope, solar radiation, and phenological stage, and a pseudothreshold functional form for distance to motorized roads. Patterns of resource selection and spatial scales of explanatory covariates of adult female elk varied among seasons (Figs. 3-4, see Appendix S5). In general, adult female elk selected areas at low to moderate elevations on moderate slopes, with higher terrain position index (i.e., on ridges) and

low to high solar radiation. Elk avoided motorized roads and snow cover, and selected agricultural landcover and intermediate values of daily NDVI (i.e., surrogate for phenology stage). Patterns of selection for forest landcover, shrub landcover, and annual integrated NDVI (i.e., surrogate for patch quality or biomass) changed among seasons; female elk selected forest landcover only during summer, shrub landcover during spring and summer, and annual integrated NDVI only during spring.

The internal predictive accuracy of our RSFs was strong; the average $r_s$ from 100 repetitions of our 5-fold cross validation procedure was 1.00 (95% range = 1.00-1.00) during all seasons. The ability of our partial RSFs to predict the space use of excluded herds was also strong. The average $r_s$ for our 24 partial RSFs was 0.98 in winter, 0.99 in spring, and 0.95 in summer (see Appendix S6).

We estimated that a minimum of 17,474 adult female elk lived within the Montana DSA, and had at least 525 abortion events within the boundary of the DSA each year during the risk period (15 February-30 June). Uncertainty associated with just the visibility bias during aerial surveys would increase the estimated number of abortion events from 525 to between 553 and 820 (assuming 95% and 64% visibility, respectively). Uncertainty associated with only the annual probability of aborting or with seroprevalence estimates would create 95% credible intervals of abortion events within the DSA to vary from 361-755 and from 436-621, respectively. We estimated that 4% of abortion events within the DSA occurred during February, 32% during March, 29% during April, 30% during May, and 5% during June (Fig. 5, see Appendix S7).

Within the risk period during an average snowfall year, we estimated that 51% of abortion events inside the Montana DSA occurred on private lands (comprising 35% of land in the DSA), 37% on USFS lands (comprising 47% of land in the DSA), 8% on state lands (comprising 8% of land in the DSA), 4% on BLM lands (comprising 8% of land in the DSA), and <1% on USFWS lands (comprising 1% of land in the DSA; Fig. 6A). However, when we limited our analyses to only include areas with potential livestock presence, we found that 98% of our estimated brucellosis-induced abortion events occurred on private ranchlands (comprising 31% of land in the DSA), 1% on state livestock allotments (comprising 1% of land in the DSA), 1% on BLM livestock allotments (comprising 4% of land in the DSA), and <1% on USFS livestock allotments (comprising 5% of land in the DSA; Fig. 6B). Note that the percentages of land in the DSA that were comprised of allotments (provided above in parentheses) were calculated only for allotments where livestock was present at some point during the risk period.

Abortion events on private ranchlands (private land with potential livestock presence) represented 49% of the total estimated abortion events that occurred during an average snowfall year within the Montana DSA. Across elk hunting districts, there was a large amount of variation in the density of abortions occurring on private ranchlands, ranging from an estimated density of <0.001 abortions / $km^2$ in hunting district 316 to an estimated density of 0.091 abortions / $km^2$ in hunting district 362 (Fig. 7A). Differences in the monthly density of abortions on private ranchlands among hunting districts were fairly consistent across time during the risk period (see Appendix S8). Across hunting districts, we also identified a large amount of variation in the estimated number of abortions individual adult female elk had on private ranchlands. During the risk period, we estimated that the average adult female elk in hunting district 301/309 had 0.002 abortions, whereas the average adult female elk in hunting district 317 had 0.040 abortions (Fig. 7B).

## Discussion

To date, few studies have attempted to synthesize movement and disease ecology (Dougherty et al. 2018). When such work has occurred, it has typically been at coarse resolutions, and has relied on a number of parameters that are poorly estimated or incompletely known (but see Merkle et al. 2018). Here, we built upon the work of Merkle et al. (2018), and developed a fine-resolution (250-m spatial, 1-day temporal), large-scale (17,732 $km^2$) disease transmission risk model that accounted for most of the measurable components of elk-to-livestock brucellosis transmission risk. There were several components of transmission risk that we were unable to consider in our model, however, because we lacked the necessary data to do so. Specifically, we did not account for contact rates of livestock with infected fetuses, how often that contact results in infection, the environmental persistence of *B. abortus*, or potential immune responses in elk or livestock that might prevent infection. Aune et al. (2012) found that brucellosis bacteria can persist on fetal tissues and soil or vegetation for 21-81 days depending on month, temperature, and exposure to sunlight, but that there was only a 0.05% chance of brucellosis surviving beyond 26 days. We expect that few aborted fetuses will persist on the landscape for that long, however, because they will likely be removed by scavengers much more quickly (Cook et al. 2004). We do not currently have estimates of fetal scavenging rates for our study area, but ongoing work to estimate the persistence of fetuses will allow us to incorporate these estimates into our framework in the future. Finally, we also did not account for potential shifts in habitat selection by adult female elk that may have occurred prior to or during parturition. We believe this likely had little impact on our results, however, because the majority of sampled elk were pregnant, and therefore, any behavioral shifts that may have occurred should have been incorporated into our RSFs.

Our results suggested that the risk of disease spillover within the Montana DSA was greatest on private ranchlands, with only ~2% of total risk occurring on state or federal grazing allotments when livestock were present on those allotments (Fig. 6B). Within the DSA, areas at higher risk for elk abortions in livestock grazing areas were concentrated along the Madison Valley in the west, and the Paradise Valley in the east (Fig. 5), which is in rough agreement with where livestock herds have been affected by brucellosis (Brennan et al. 2017). Our findings contrast with those of Merkle et al. (2018), who found that elk abortion events in Wyoming were primarily concentrated on USFS lands, with private lands estimated to play a minimal role in transmission risk. These differences between states highlight one of the challenges of managing brucellosis in the GYE: intervention strategies will likely need to be site-specific to be most effective.

Our work identified areas of high transmission risk (Fig. 5, Fig. 7A, see Appendix S7), and may be used to optimize disease mitigation efforts across space and time. Traditional methods of disease control, such as vaccination, culling, and test and slaughter, are unlikely to be effective, politically feasible, or logistically possible to implement on wide-ranging elk populations (Bienen and Tabor 2006, Kilpatrick et al. 2009). Thus, the primary strategy for managing brucellosis transmission risk between elk and livestock is to prevent commingling. This may be achieved by hiring herders to disperse or redistribute elk, by holding dispersal hunts, by fencing or removing haystacks and other attractants, or by improving available forage on public lands (Bienen and Tabor 2006).

Our results indicated that individual female elk posed different per-capita levels of brucellosis transmission risk because of differences in seroprevalence, movement patterns, and landownership among hunting districts. For example, we predicted that one female elk in hunting

district 317 generated 4 times more risk on private ranchlands than one in hunting district 313 (Fig. 7B), primarily due to differences in seroprevalence and landownership. Hunting districts with the highest per-capita risk of brucellosis transmission from elk to livestock on private ranchlands were not always the hunting districts with the highest densities of abortions on private ranchlands (Fig. 6). For most management interventions, the greatest overall reduction in risk will likely be achieved by focusing on hunting districts with the highest density of abortions. Currently, there is no limit on the total number of elk that can be targeted during management interventions in Montana. If logistical, financial, or social constraints limit the total number of elk that can be targeted in the future, however, it may be useful for managers to consider both risk metrics (per-capita, density) when designing mitigation strategies.

We expanded upon the work of Merkle et al. (2018) by incorporating spatiotemporal data of livestock distribution into our modeling framework. In doing so, we demonstrated the importance of considering livestock distribution during investigations of elk-to-livestock brucellosis spillover. By itself, the distribution of abortions across landownership types did not provide an accurate picture of the distribution of transmission risk. For example, we estimated that 51% of abortions occurred on private lands, and 37% occurred on USFS lands (Fig. 6A). When we considered the spatiotemporal distribution of livestock, however, we found that elk-to-livestock transmission risk was primarily concentrated on private ranchlands, with 98% of brucellosis-induced abortion events on livestock grazing lands occurring on private ranchlands (Fig. 6B). It is important to note, however, that we lacked detailed data on the spatiotemporal distribution of livestock on private ranchlands. As a result, we most likely overestimated risk on private ranchlands because we assumed that livestock were always present on this grazing type. Further, we were unable to account for the number of livestock and the chance that livestock may be infected by a given elk fetus, so our gradient of risk may be only weakly correlated with the occurrence of actual spillover events. Nonetheless, our results are reflective of differences in transmission risk posed by elk across the landscape.

The current stocking dates for livestock on state and federal allotments within the Montana DSA appear to be effective at limiting commingling of elk and livestock during the risk period. Recently, however, Kamath et al. (2016) estimated that the distribution of brucellosis in elk in the GYE is expanding at 3-8 km per year and that the rate of expansion appeared to increase over time. Outside the northern boundary of the Montana DSA the density of BLM allotments that are stocked with livestock during the risk period is much higher. If brucellosis continues to expand this may become an important issue.

Within the DSA, uncertainty associated with the timing of abortions had the largest influence on the predicted number and density of abortions. The model of abortion phenology we employed was developed in Wyoming by Cross et al. (2015), using data from vaginal implant transmitters deployed in 575 elk from 2006-2014. It is unlikely that a similar dataset will be replicated in the near future, due to the high cost and logistical demands required to assemble a sample of similar or greater size. Therefore, it may be unrealistic to target abortion phenology in data collection and surveillance strategies to attempt to minimize uncertainty in risk predictions. Instead, developing a model to correct for visibility bias (Samuel et al. 1987) during aerial surveys, the 2$^{nd}$ largest contributor to uncertainty, might be a more feasible way to reduce overall uncertainty. Increased efforts to refine brucellosis serology estimates might also help to reduce overall uncertainty. Additionally, as computational capacity increases in the future, it may be useful to account for the unknown uncertainty associated with space-use predictions. Further research is needed, however, to assess whether or not reductions in uncertainty are useful for

focusing efforts aimed at reducing transmission risk (i.e., assessing whether or not reductions in uncertainty alter predicted differences in risk among areas).

Because management decisions for elk in areas with brucellosis in Montana are made annually, our modeling approach could be used in the design of an Adaptive Management program whereby uncertainty in predictions could be reduced over time (Walters 1986). The value of this approach, versus annual state-dependent decision making, depends on the extent to which the uncertainty we documented affects wildlife managers' choice among the portfolio of elk distribution management options available. Expected value-of-information analyses could be used to estimate the extent to which the brucellosis management program for elk could be improved by implementation of Adaptive Management to reduce uncertainty in the risk of elk-to-livestock transmission (*sensu* Runge et al. 2011).

The number of brucellosis-induced abortions from elk involves complex interactions among the demographic, seroprevalence, and space use patterns of elk, as well as the timing of abortion events (National Academies of Sciences, Engineering, and Medicine 2017). Our dataset did not permit us to account for these interactions equally across the DSA, however. We had detailed movement data for some elk herds, which allowed us to distribute the estimated number of adult female elk from those herds among the hunting districts of the DSA according to the movement patterns of collared females (see Appendix S3). Conversely, in hunting districts without movement data, we had to assume that the number of female elk was static throughout the risk period (unless sampled herds moved into these hunting districts). This likely biased our estimates of abortion events high in some hunting districts (i.e., HD 323) because elk likely departed the district during the risk period. In other hunting districts, there was likely little movement outside of the district (i.e., HD 301), so we expect that this issue likely had little effect. During future collaring efforts, it may be beneficial to target hunting districts without recent movement data where elk-to-livestock brucellosis transmission risk estimates are high (i.e., hunting districts 323 and 360; Fig. 6).

Across disciplines, synthesizing data collected at different spatial scales is challenging (Gotway and Young 2002). We collected brucellosis seroprevalence data at the scale of the hunting district from hunter-harvested and research-captured adult female elk (see Appendix S3). Because most of our seroprevalence estimates could not be coupled with individual elk herds, we could not adjust seroprevalence estimates according to the movement patterns of collared females. Among hunting districts, we observed a large amount of variation in transmission risk (Fig. 7A, see Appendix S7). We are confident that much of this variation was due to true biological differences among hunting districts. We are aware, however, that some of this variation was likely artificially introduced because of the scale at which our seroprevalence data were collected. For example, abrupt changes in the predicted number of abortions along some hunting district borders (e.g., border of hunting district 323 and 330; see Appendix S7) likely did not represent biological reality on the ground.

**Management implications**

In Montana, management decisions for elk in the DSA are made annually by the Montana Fish and Wildlife Commission and are guided by a Structured Decision Making framework (Montana Fish, Wildlife and Parks 2013). A fundamental objective of this management program is to minimize the risk of brucellosis transmission from elk to livestock. Management actions to achieve this objective are focused on hazing, hunting, and other actions to disperse or redistribute elk. Our integrated modeling approach was designed to feed directly into this management

program as a tool to prioritize when and where to implement these interventions. Our results suggest that brucellosis transmission risk from elk to livestock in Montana is greatest from March through May on private ranchlands. Focusing management activities on private ranchlands during these periods of highest risk will likely reduce disease spillover opportunities. Managers could also use our results to provide quantitative predictions of the expected reduction in transmission risk that might follow from a set of elk distribution management actions employed in a given year. Such predictions and assessments should be conducted in the context of similar evaluations for other fundamental objectives related to stakeholder acceptance of management actions and costs of implementation (Metcalf et al. 2017). Additionally, we suggest that wildlife managers and livestock producers collaboratively gather data on the distribution of livestock on private ranchlands during the brucellosis transmission risk period. These data could then be used to refine estimates of where transmission events from elk to livestock are most likely to occur on private ranchlands.

**Acknowledgements**

Funding was provided by the U.S. Geological Survey and Montana Fish, Wildlife and Parks (FWP) through an agreement with Montana Department of Livestock and the Animal and Plant Health Inspection Service of the U.S. Department of Agriculture. We thank the many FWP staff for their efforts in helping with landowner contacts, field operations, and continued support of this project. We thank pilots N. Cadwell, B. Malo, M. Shelton, M. Stott, and R. Swisher for their work in capturing elk. We thank F. Thompson and the Bureau of Land Management (BLM) for compiling the BLM livestock allotment data. We thank S. Wells, L. McNew, D. Tyers, and the U.S. Forest Service (USFS) forest supervisors of the Greater Yellowstone Ecosystem for assembling the USFS livestock allotment data. We thank J. Cunningham, K. Loveless, and D. Waltee for their work collecting elk count data. We thank A. Brennan, K. Szcodronski, and K. Manlove for helpful discussions about this work. We thank Q. Kujala for helpful comments that improved this manuscript and for securing the funding to conduct this work. We thank K. Haase and G. Bastille-Rousseau for valuable comments that improved this manuscript. Any use of trade, firm, or product names is for descriptive purposes only and does not imply endorsement by the U.S. Government.

**Literature Cited**

Anderson, C. R. J., D. S. Moody, B. L. Smith, F. G. Lindzey, and R. P. Lanka. 1998. Development and evaluation of sightability models for summer elk surveys. Journal of Wildlife Management 62:1055–1066.

Aune, K., J. C. Rhyan, R. Russell, T. J. Roffe, and B. Corso. 2012. Environmental persistence of Brucella abortus in the Greater Yellowstone Area. Journal of Wildlife Management 76:253–261.

Bienen, L., and G. Tabor. 2006. Applying an ecosystem approach to brucellosis control: can an old conflict between wildlife and agriculture be successfully managed? Frontiers in Ecology and the Environment 4:319–327.

Bischof, R., L. E. Loe, E. L. Meisingset, B. Zimmermann, B. Van Moorter, and A. Mysterud. 2012. A migratory northern ungulate in the pursuit of spring: jumping or surfing the green wave? American Naturalist 180:407–424.

Bolker, B. M., M. E. Brooks, C. J. Clark, S. W. Geange, J. R. Poulsen, M. H. H. Stevens, and J.-S. S. White. 2009. Generalized linear mixed models: a practical guide for ecology and evolution. Trends in Ecology and Evolution 24:127–135.

Boyce, M. S., P. R. Vernier, S. E. Nielsen, and F. K. A. Schmiegelow. 2002. Evaluating resource selection functions. Ecological Modelling 157:281–300.

Brennan, A., P. C. Cross, K. Portacci, B. M. Scurlock, and W. H. Edwards. 2017. Shifting brucellosis risk in livestock coincides with spreading seroprevalence in elk. PLoS ONE 12:e0178780.

Burnham, K. P., and D. R. Anderson. 2002. Model selection and multimodel inference: a practical information-theoretic approach. Springer, New York, New York, USA.

Cheville, N. F., D. R. McCullough, and L. R. Paulson. 1998. Brucellosis in the greater Yellowstone area. National Academy Press, Washington, D.C., USA.

Conover, M. 2001. Resolving human-wildlife conflicts: the science of wildlife damage management. CRC Press, Boca Raton, FL, USA.

Cook, W. E., E. S. Williams, and S. A. Dubay. 2004. Disappearance of bovine fetuses in northwestern Wyoming. Wildlife Society Bulletin 32:254–259.

Cross, P. C., E. J. Maichak, A. Brennan, B. M. Scurlock, J. Henningsen, and G. Luikart. 2013. An ecological perspective on *Brucella abortus* in the western United States. Scientific and Technical Review of the Office International des Epizooties 32:79–87.

Cross, P. C., E. J. Maichak, J. D. Rogerson, K. M. Irvine, J. D. Jones, D. M. Heisey, W. H. Edwards, and B. M. Scurlock. 2015. Estimating the phenology of elk brucellosis transmission with hierarchical models of cause-specific and baseline hazards. Journal of Wildlife Management 79:739–748.

Daszak, P., A. A. Cunningham, and A. D. Hyatt. 2000. Emerging infectious diseases of wildlife— threats to biodiversity and human health. Science 287:443–449.

Diekmann, O., H. Heesterbeek, and T. Britton. 2012. Mathematical tools for understanding infectious disease dynamics. Princeton University Press, Princeton, NJ, USA.

Dormann, C. F., J. Elith, S. Bacher, C. Buchmann, G. Carl, G. Carré, J. R. García Marquéz, B. Gruber, B. Lafourcade, P. J. Leitão, T. Münkemüller, C. McClean, P. E. Osborne, B. Reineking, B. Schröder, A. K. Skidmore, D. Zurell, and S. Lautenbach. 2013. Collinearity: a review of methods to deal with it and a simulation study evaluating their performance. Ecography 36:027–046.

Dougherty, E. R., D. P. Seidel, C. J. Carlson, O. Spiegel, and W. M. Getz. 2018. Going through the motions: incorporating movement analyses into disease research. Ecology Letters 21:588–604.

Gillies, C. S., M. Hebblewhite, S. E. Nielsen, M. A. Krawchuk, C. L. Aldridge, J. L. Frair, D. J. Saher, C. E. Stevens, and C. L. Jerde. 2006. Application of random effects to the study of resource selection by animals. Journal of Animal Ecology 75:887–898.

Gotway, C. A., and L. J. Young. 2002. Combining incompatible spatial data. Journal of the American Statistical Association 97:632–648.

Graham, M. H. 2003. Confronting multicollinearity in ecological multiple regression. Ecology 84:2809–2815.

Haggerty, J. H., K. Epstein, M. Stone, and P. C. Cross. 2018. Land use diversification and intensification on elk winter range in Greater Yellowstone: framework and agenda for social-ecological research. Rangeland Ecology and Management 71:171–174.

Hall, D. K., G. A. Riggs, V. V. Salomonson, N. E. DiGirolamo, and K. J. Bayr. 2002. MODIS snow-cover products. Remote Sensing of Environment 83:181–194.

Jarding, A. R. 2010. Population estimation procedures for elk and deer in the black hills, South Dakota: development of sightability model and spotlight survey. M.S. thesis, South Dakota State University, Brookings, South Dakota, USA.

Kamath, P. L., J. T. Foster, K. P. Drees, G. Luikart, C. Quance, N. J. Anderson, P. R. Clarke, E. K. Cole, M. L. Drew, W. H. Edwards, J. C. Rhyan, J. J. Treanor, R. L. Wallen, P. J. White, S. Robbe-Austerman, and P. C. Cross. 2016. Genomics reveals historic and contemporary transmission dynamics of a bacterial disease among wildlife and livestock. Nature Communications 7:11448.

Kays, R., M. C. Crofoot, W. Jetz, and M. Wikelski. 2015. Terrestrial animal tracking as an eye on life and planet. Science 348:aaa2478.

Kilpatrick, A. M., C. M. Gillin, and P. Daszak. 2009. Wildlife-livestock conflict: the risk of pathogen transmission from bison to cattle outside Yellowstone National Park. Journal of Applied Ecology 46:476–485.

Laforge, M. P., E. Vander Wal, R. K. Brook, E. M. Bayne, and P. D. McLoughlin. 2015. Process-focussed, multi-grain resource selection functions. Ecological Modelling 305:10–21.

Madden, F. 2004. Creating coexistence between humans and wildlife: global perspectives on local efforts to address human-wildlife conflict. Human Dimensions of Wildlife 9:247–257.

Manly, B. F. J., L. L. McDonald, D. L. Thomas, T. L. McDonald, and W. P. Erickson. 2002. Resource selection by animals: statistical design and analysis for field studies. Second edition. Kluwer Academic Publishers, Dordrecht, The Netherlands.

Merkle, J. A., P. C. Cross, B. M. Scurlock, E. K. Cole, A. B. Courtemanch, S. R. Dewey, and M. J. Kauffman. 2018. Linking spring phenology with mechanistic models of host movement to predict disease transmission risk. Journal of Applied Ecology 55:810–819.

Merkle, J. A., K. L. Monteith, E. O. Aikens, M. M. Hayes, K. R. Hersey, A. D. Middleton, B. A. Oates, H. Sawyer, B. M. Scurlock, and M. J. Kauffman. 2016. Large herbivores surf waves of green-up in spring. Proceedings of the Royal Society B 283:20160456.

Merkle, J. A., J. R. Potts, and D. Fortin. 2017. Energy benefits and emergent space use patterns of an empirically parameterized model of memory-based patch selection. Oikos 126:185–195.

Metcalf, A. L., E. C. Metcalf, K. Khumalo, J. Gude, Q. Kujala, and M. S. Lewis. 2017. Public wildlife management on private lands: reciprocity, population status, and stakeholders' normative beliefs. Human Dimensions of Wildlife 22:564–582.

Meyer, C. B., and W. Thuiller. 2006. Accuracy of resource selection functions across spatial scales.

Montana Fish, Wildlife and Parks. 2013. Elk management guidelines in areas with brucellosis working group proposed final recommendations. Helena, MT, USA.

Montana Fish, Wildlife and Parks. 2015. Targeted elk brucellosis surveillance project 2011-2015 comprehensive report. Helena, MT, USA.

National Academies of Sciences, Engineering, and Medicine. 2017. Revisiting brucellosis in the Greater Yellowstone Area. The National Academies Press, Washington, D.C., USA.

Nishi, J. S., T. Shury, and B. T. Elkin. 2006. Wildlife reservoirs for bovine tuberculosis (*Mycobacterium bovis*) in Canada: strategies for management and research. Veterinary Microbiology 112:325–338.

Pappas, G., P. Papadimitriou, N. Akritidis, L. Christou, and E. V. Tsianos. 2006. The new global map of human brucellosis. Lancet Infectious Diseases 6:91–99.

Pettorelli, N., J. O. Vik, A. Mysterud, J.-M. Gaillard, C. J. Tucker, and N. C. Stenseth. 2005. Using the satellite-derived NDVI to assess ecological responses to environmental change. Trends in Ecology and Evolution 20:503–510.

Potts, J. R., G. Bastille-Rousseau, D. L. Murray, J. A. Schaefer, and M. A. Lewis. 2014. Predicting local and non-local effects of resources on animal space use using a mechanistic step selection model. Methods in Ecology and Evolution 5:253–262.

Proffitt, K. M., N. Anderson, P. Lukacs, M. M. Riordan, J. A. Gude, and J. Shamhart. 2015. Effects of elk density on elk aggregation patterns and exposure to brucellosis. Journal of Wildlife Management 79:373–383.

Proffitt, K. M., J. A. Gude, K. L. Hamlin, R. A. Garrott, J. A. Cunningham, and J. L. Grigg. 2011. Elk distribution and spatial overlap with livestock during the brucellosis transmission risk period. Journal of Applied Ecology 48:471–478.

Prokopenko, C. M., M. S. Boyce, and T. Avgar. 2017. Extent-dependent habitat selection in a migratory large herbivore: road avoidance across scales. Landscape Ecology 32:313–325.

R Development Core Team. 2016. R: a language and environment for statistical computing. Vienna, Austria.

Ragan, V. E. 2002. The Animal and Plant Health Inspection Service (APHIS) brucellosis eradication program in the United States. Veterinary Microbiology 90:11–18.

Ranglack, D. H., K. M. Proffitt, J. E. Canfield, J. A. Gude, J. Rotella, and R. A. Garrott. 2017. Security areas for elk during archery and rifle hunting seasons. Journal of Wildlife Management 81:778–791.

Rhyan, J. C., P. Nol, C. Quance, A. Gertonson, J. Belfrage, L. Harris, K. Straka, and S. Robbe-Austerman. 2013. Transmission of brucellosis from elk to cattle and bison, Greater Yellowstone Area, USA, 2002-2012. Emerging Infectious Diseases 19:1992–1995.

Runge, M. C., S. J. Converse, and J. E. Lyons. 2011. Which uncertainty? Using expert elicitation and expected value of information to design an adaptive program. Biological Conservation 144:1214–1223.

Samuel, M. D., E. O. Garton, M. W. Schlegel, and R. G. Carson. 1987. Visibility bias during aerial surveys of elk in northcentral Idaho. Journal of Wildlife Management 51:622–630.

Sitati, N. W., M. J. Walpole, R. J. Smith, and N. Leader-Williams. 2003. Predicting spatial aspects of human and elephant conflict. Journal of Applied Ecology 4:667–677.

Walters, C. J. 1986. Adaptive management of renewable resources. Macmillan, New York, New York, USA.

Wells, S. L. 2017. Livestock depredation by grizzly bears on Forest Service grazing allotments in the Greater Yellowstone Ecosystem. M.S. thesis, Montana State University, Bozeman, MT, USA.

White, L. A., J. D. Forester, and M. E. Craft. 2017. Dynamic, spatial models of parasite transmission in wildlife: their structure, applications, and remaining challenges. Journal of Animal Ecology.

White, P. J., K. M. Proffitt, L. D. Mech, S. B. Evans, J. A. Cunningham, and K. L. Hamlin. 2010. Migration of northern Yellowstone elk: implications of spatial structuring. Journal of Mammalogy 91:827–837.

Woodroffe, R., S. Thirgood, and A. Rabinowitz, editors. 2005. People and wildlife, conflict or coexistence? Cambridge University Press, Cambridge, United Kingdom.

Zidon, R., S. Garti, W. M. Getz, and D. Saltz. 2017. Zebra migration strategies and anthrax in Etosha National Park, Namibia. Ecosphere 8:e01925.

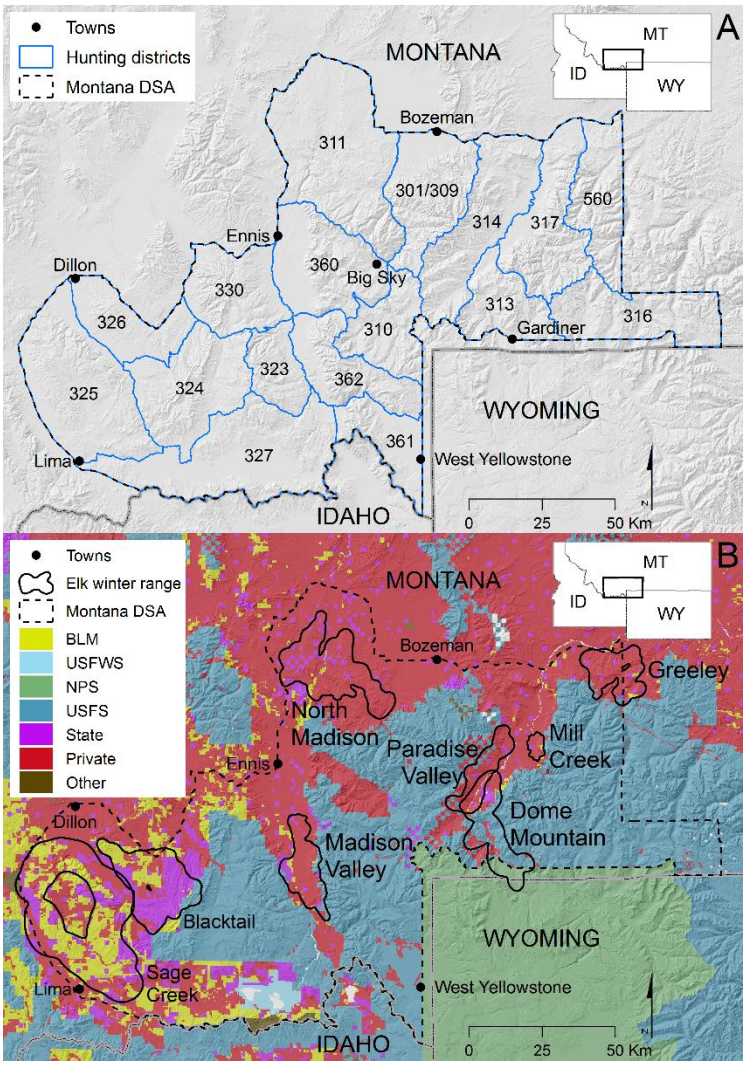


**Figure 1. (A)** Elk hunting districts (HDs; labeled with black text) within the Montana designated brucellosis surveillance area (DSA; black dashed line). Note that HD 301 and HD 309 were merged in our analyses (see Methods), and the portion of HDs 301/309, 311, 316, and 560 that extend beyond the border of the DSA are not shown. Shading depicts hillshade of elevation. **(B)** Winter ranges of 8 elk herds (labeled with black text) within the Montana DSA where adult female elk were radiocollared, and the matrix of Bureau of Land Management (BLM), U.S. Fish and Wildlife Service (USFWS), National Park Service (NPS), U.S. Forest Service (USFS), state government (State), private (Private), and other (Other) lands in the region. Shading depicts hillshade of elevation.

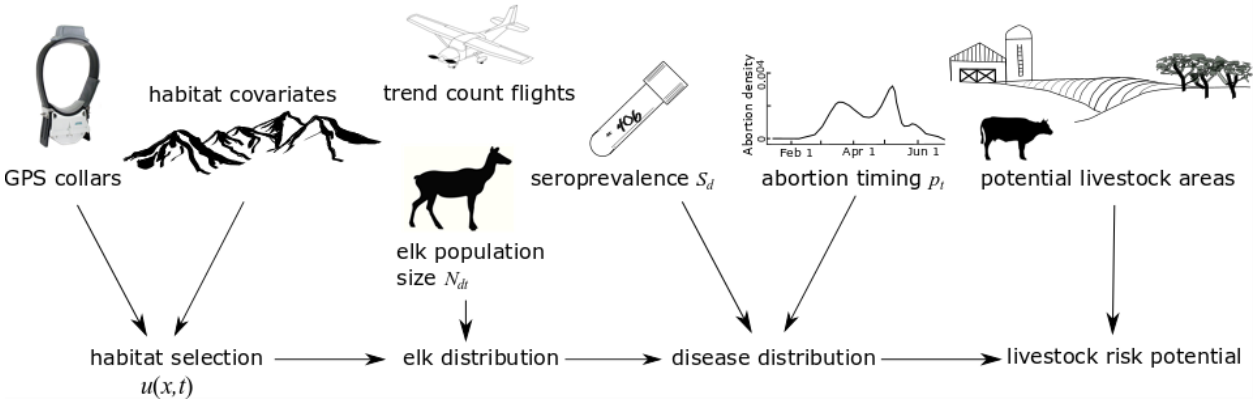


**Figure 2.** Decomposition of the analysis of elk-to-livestock brucellosis transmission risk into its constituent parts.

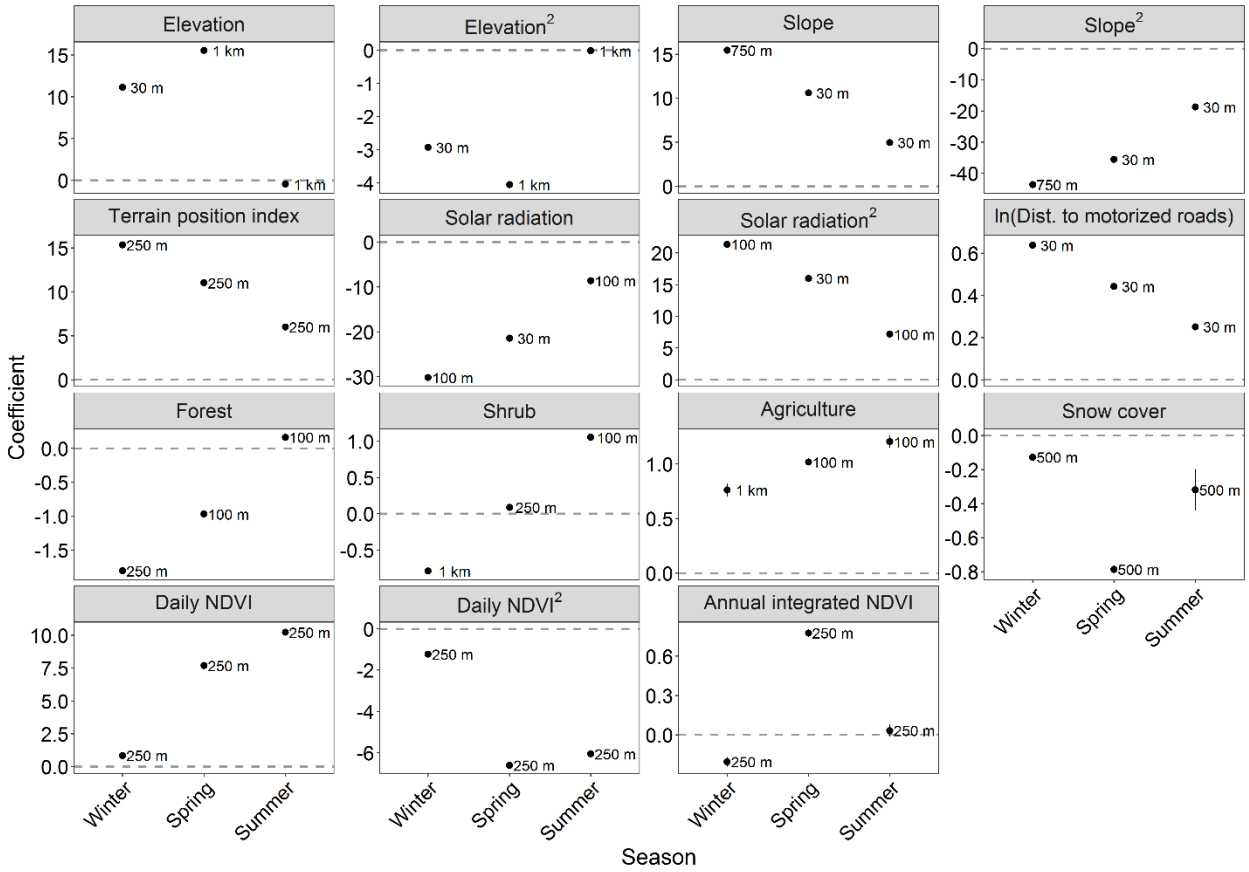


**Figure 3.** Estimated coefficients and 95% confidence intervals from resource selection functions for adult female elk during winter (15 February-31 March), spring (1 April-31 May), and summer (1 June-30 June) seasons in southwest Montana, USA. The scale for each variable in meters (m) or kilometers (km) is given to the right of each estimated coefficient. The dashed line in each panel represents an estimated selection coefficient of 0.

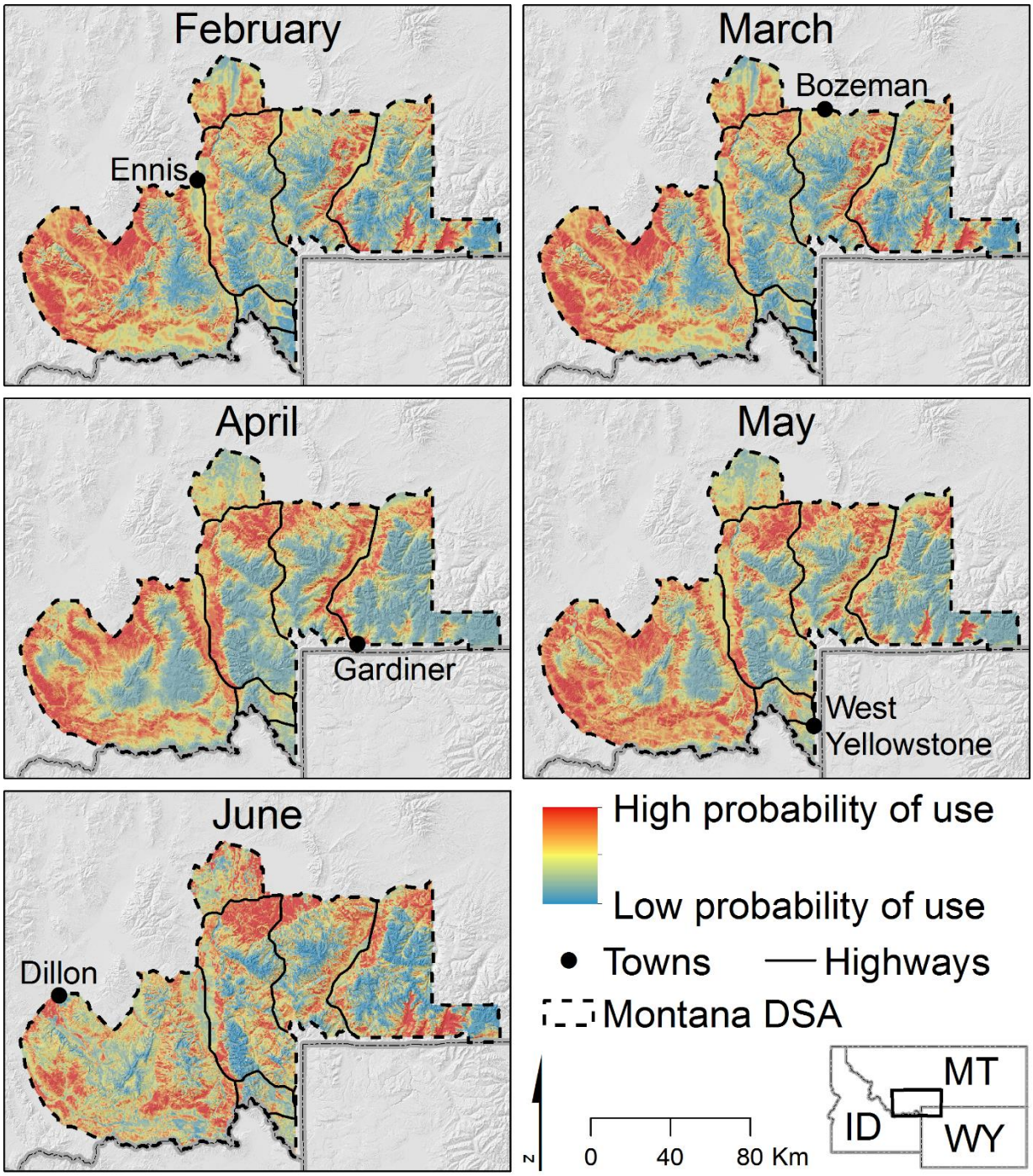


**Figure 4.** Predicted relative probability of use by adult female elk within the boundary of the Montana designated brucellosis surveillance area (DSA) during each month of the brucellosis transmission risk period (15 February-30 June). Monthly estimates were produced by summing daily estimates of the relative probability of use during all days of the month. Shading depicts hillshade of elevation.

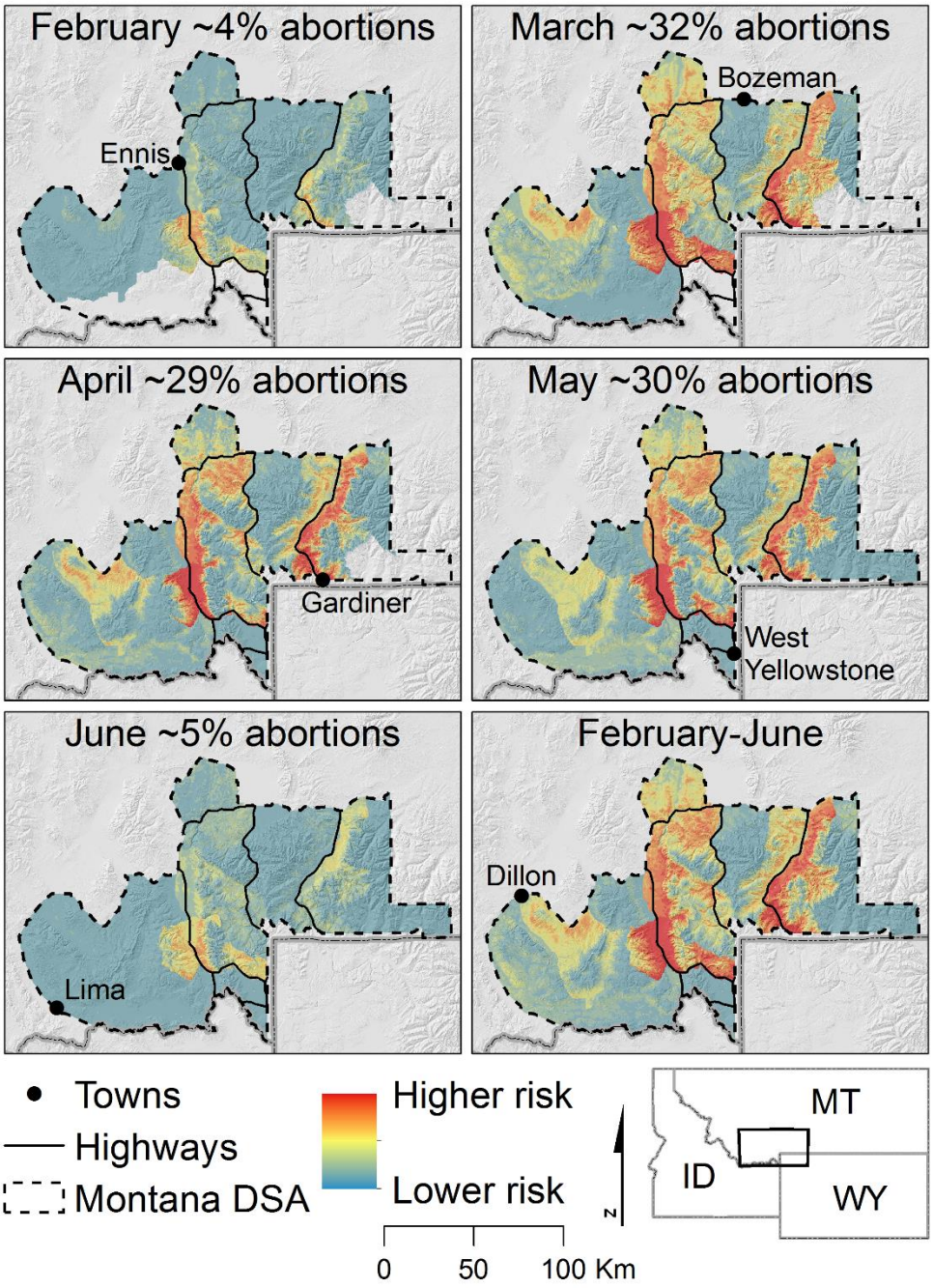


**Figure 5.** Predicted risk of brucellosis-induced abortion events by adult female elk within the boundary of the Montana designated brucellosis surveillance area (DSA) during each month of the brucellosis transmission risk period (15 February-30 June). Monthly estimates were produced by summing daily estimates of the risk of abortion events during all days of the month. Shading depicts hillshade of elevation.

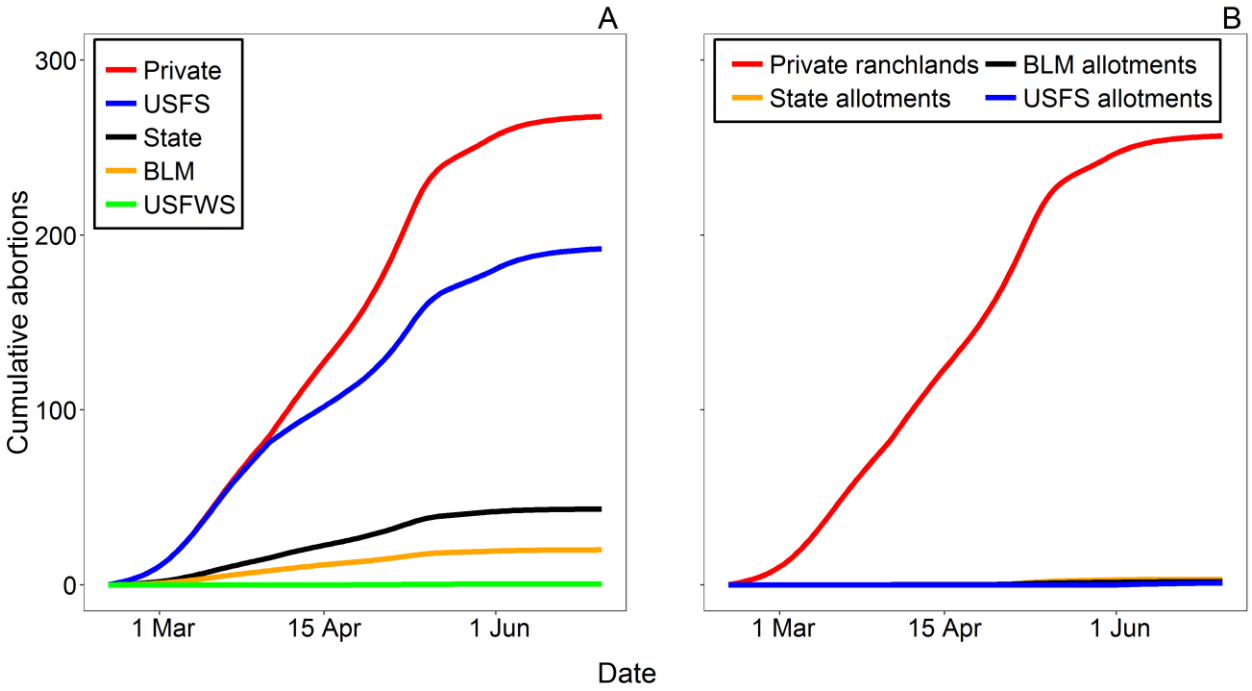


**Figure 6.** Daily predicted number of cumulative brucellosis-induced abortion events from adult female elk within the Montana designated brucellosis surveillance area (DSA) during the brucellosis transmission risk period (15 February-30 June) occurring on **(A)** private (Private), U.S. Forest Service (USFS), state government (State), Bureau of Land Management (BLM), and U.S. Fish and Wildlife Service (USFWS) lands, and on **(B)** livestock grazing lands (private ranchlands and state and federal livestock allotments) when livestock were present.

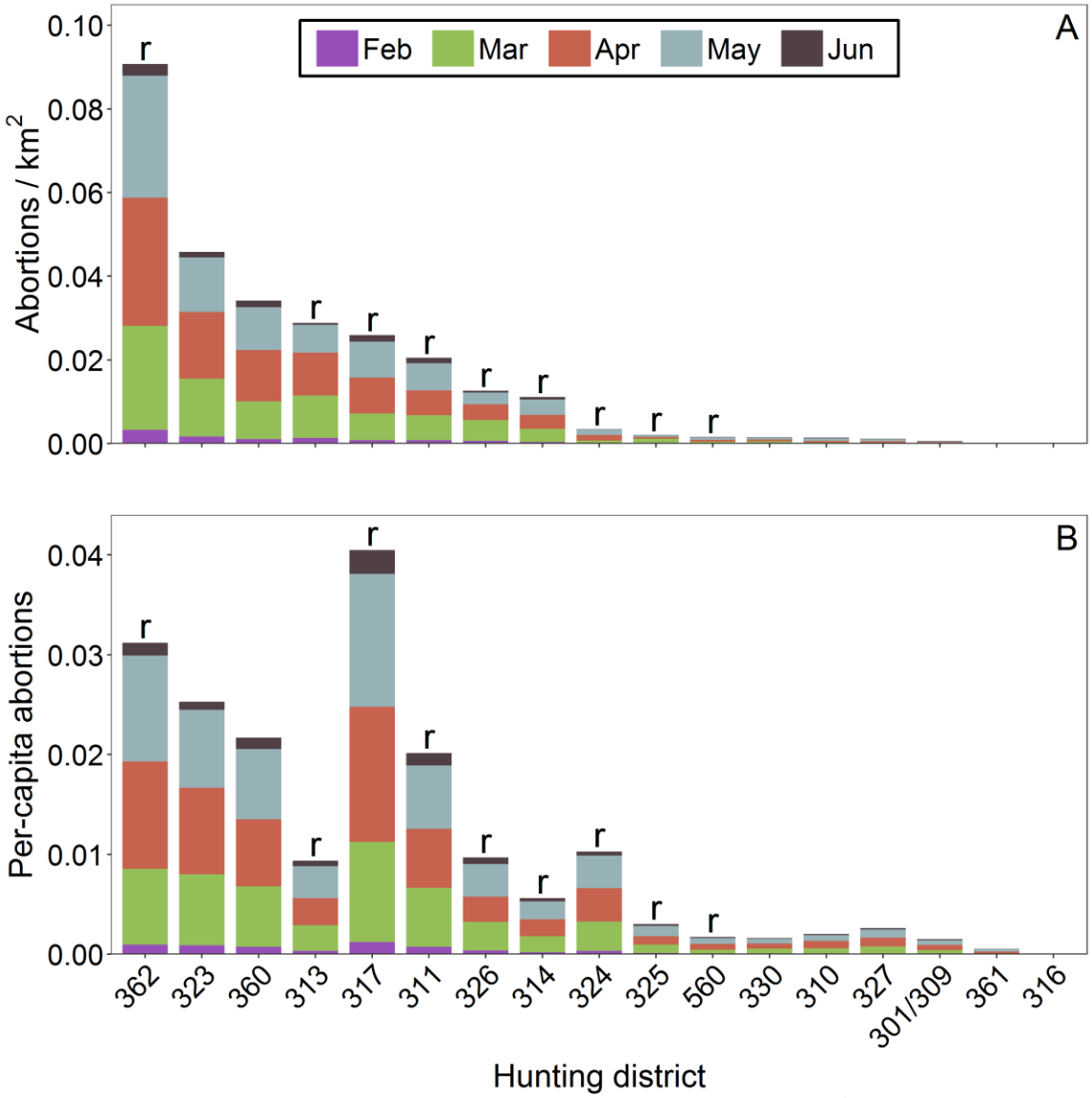


**Figure 7. (A)** Predicted monthly density of abortions (abortions / km$^2$) on private ranchlands, and **(B)** predicted monthly number of per-capita cumulative abortions (cumulative abortions per hunting district / adult female elk count per hunting district) occurring on private ranchlands. The density of abortions and the per-capita cumulative abortions were calculated for the portion of elk hunting districts that fall within the boundary of the Montana designated brucellosis surveillance area (DSA) during the brucellosis transmission risk period (15 February-30 June). Hunting districts where adult female elk were radiocollared are indicated by an 'r' at the top of the bars.

**APPENDIX S1.** Spatial scales evaluated for each variable in resource selection functions.

**Table S1.** The spatial scales evaluated for all non-time-vary variables (except distance to motorized roads) in resource selection functions of adult female elk in southwest Montana, USA. For each variable, we iteratively calculated moving window averages (at the resolution of the original data) within concentric radii (30, 100, 250, 500, 750, 1,000 m) larger than the resolution of the original data.

| Variable | Spatial scales (m) |
|---|---|
| Elevation | 30, 100, 250, 500, 750, 1,000 |
| Slope | 30, 100, 250, 500, 750, 1,000 |
| Terrain position index | 30, 100, 250, 500, 750, 1,000 |
| Solar radiation | 30, 100, 250, 500, 750, 1,000 |
| Forest | 30, 100, 250, 500, 750, 1,000 |
| Shrub | 30, 100, 250, 500, 750, 1,000 |
| Agriculture | 30, 100, 250, 500, 750, 1,000 |
| Annual integrated NDVI | 250, 500, 750, 1,000 |

**APPENDIX S2.** Method for estimating average snowfall year.

We downloaded snow water equivalent (SWE) data from 19 SNOTEL sites (U.S. Department of Agriculture, Natural Resources Conservation Service) located within the Montana designated surveillance area (DSA) for brucellosis during all years that elk were monitored (2005-2015). At each site in each year, we calculated the cumulative SWE value from 1 October-30 April. Because of the variation in cumulative SWE values among sites, we calculated a SWE anomaly for each site in each year. We calculated the cumulative SWE anomaly by subtracting the mean cumulative SWE value from 2005-2015 for individual sites from the cumulative SWE value for each site in each year. We then identified a representative year for average snowfall (2013) from among the years of elk monitoring (Fig. S1).

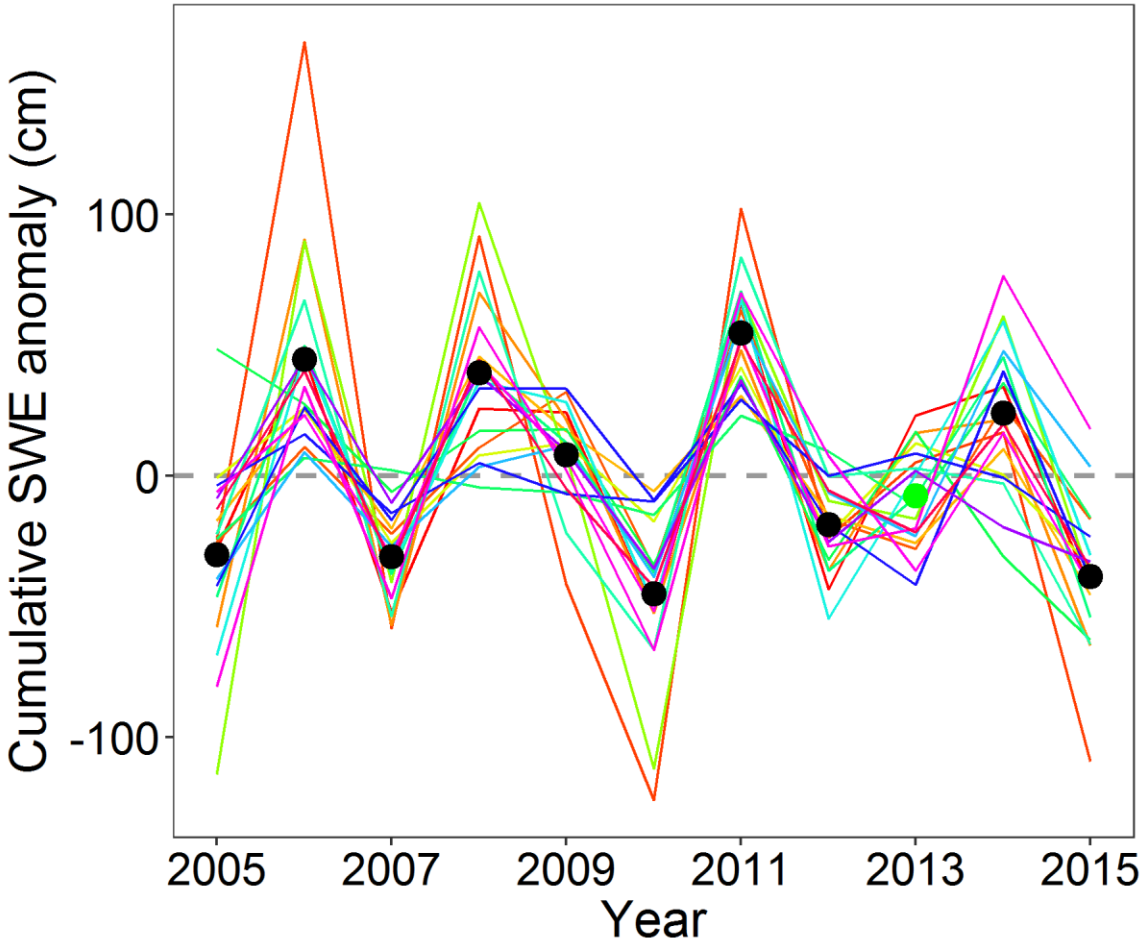


**Figure S1.** Cumulative snow water equivalent (SWE) anomaly from 1 October-30 April for 19 SNOTEL sites located within the Montana designated surveillance area for brucellosis from 2005-2015. Each SNOTEL site is represented by a line. The average cumulative SWE anomaly in each year is shown by filled circles, with the representative average snowfall year among the years of monitoring identified (green circle; 2013).

**APPENDIX S3.** Female elk abundance and brucellosis seroprevalence data.

Each winter, the Montana Department of Fish, Wildlife and Parks (FWP) collects elk survey data on winter range (Fig. S1; see Proffitt et al. 2015 for additional details). We averaged calf:female ratios from the 3 most recent years of survey data to estimate the number of elk calves per 100 adult females *c* (this ratio is not estimated every year), and we assumed the number of adult male elk per 100 adult females *m* was 10 for all herds (Montana Fish, Wildlife and Parks, unpublished data). We estimated the proportion of adult female elk *z* as:

$$z = 1 - \left(\frac{c + m}{100 + c + m}\right) \quad (1)$$

We had detailed movement data for 8 elk herds within the Montana designated brucellosis surveillance area (DSA) where we had captured and deployed Global Positioning System (GPS) collars on adult female elk ≥2 years of age. We distributed the estimated number of adult female elk from these sampled herds among the hunting districts of the DSA according to the movement patterns of collared females. Because we lacked movement data for unsampled herds, we assumed that unsampled herds remained within the hunting district where they were counted during winter surveys. We merged hunting district 301 and hunting district 309 into one district (i.e., hunting district 301/309) because these districts were treated as one unit during winter surveys. We defined **M** as a matrix with *h* rows and *d* columns, with cells containing the proportion of sampled herd *h* (i.e., a herd with GPS location data) located within the portion of elk hunting district *d* that was within the boundary of the DSA. To estimate the daily proportion of time each sampled herd was located within each hunting district (**M** cell values), we estimated the time individual collared elk were within the borders of each hunting district in each day, and averaged those values (Fig. S2). We estimated the number of adult female elk $f(d, t)$ in the portion of each hunting district *d* that was within the boundary of the DSA per time step *t* (in days) as:

$$f(d,t) = z_d u_d + \mathbf{M}_t z_h s_h \quad (2)$$

where $u_d$ is the population estimate of unsampled elk (i.e., herds with no location data from GPS collars) in hunting district *d* (Table S1), and $s_h$ is the population estimate of sampled elk herd *h* located in hunting district *d* during time step *t* (Table S2). We used data from the most recent surveys available (2016 or 2017) for $u_d$ and $s_h$.

In 2011, FWP initiated a multi-year brucellosis surveillance project. Personnel from FWP tested hunter-harvested and research-captured adult female elk from herds in southwest Montana for exposure to *Brucella abortus* as part of this project. Where available, we used the proportion of positive to negative results from these tests during 2011-2017 to estimate the seroprevalence of hunting districts located within the DSA (see Montana Fish, Wildlife and Parks [2015] for details on how serostatus was determined). For hunting districts without data from this project, we used seroprevalence estimates for 2014 estimated from models predicting the trend in seroprevalence over time, which were built using data collected from a combination of hunter-harvested and research-captured adult female elk (Table S3, Fig. S3; Brennan et al. 2017).

**Literature Cited**

Brennan, A., P. C. Cross, K. Portacci, B. M. Scurlock, and W. H. Edwards. 2017. Shifting brucellosis risk in livestock coincides with spreading seroprevalence in elk. PLoS ONE 12:e0178780.

Montana Fish, Wildlife and Parks. 2015. Targeted elk brucellosis surveillance project 2011-2015 comprehensive report. Montana Fish, Wildlife and Parks, Helena, MT, USA.

Proffitt, K. M., N. Anderson, P. Lukacs, M. M. Riordan, J. A. Gude, and J. Shamhart. 2015. Effects of elk density on elk aggregation patterns and exposure to brucellosis. Journal of Wildlife Management 79:373–383.

**Table S1.** Trend counts for unsampled elk (i.e., herds with no location data from Global Positioning System [GPS] collars) located within the portion of elk hunting districts that fall within the boundary of the Montana designated brucellosis surveillance area (DSA) in southwest Montana, USA, with the 3-year average calf:female ratio, and the years of survey data contributing to the estimate of the average calf:female ratio. For hunting districts containing no elk herds during winter, NA values are given. Values of 0 in the "unsampled count" column indicate that GPS collars were deployed on all elk herds within that hunting district.

| Hunting district ($d$) | Calves:100 females ($c$) | Survey years (calves:100 females) | Unsampled count ($u_d$) |
|---|---|---|---|
| 314 | 35.7 | 2014[a] | 2,306 |
| 360 | 25.0 | 2016[a] | 1,963 |
| 323 | 32.7 | 2010, 2013-2014 | 1,105 |
| 330 | 32.7 | 2010, 2013-2014 | 1,084 |
| 326 | 32.7 | 2010, 2013-2014 | 673 |
| 301/309 | 32.5 | 2010-2011[a] | 552 |
| 310 | 14.4 | 2011-2013 | 425 |
| 317 | 32.0 | 2011[a] | 185 |
| 311 | 30.0 | 2016[a] | 0 |
| 313 | 26.0 | 2015-2017 | 0 |
| 316 | NA | NA | 0 |
| 324 | 32.7 | 2010, 2013-2014 | 0 |
| 325 | 32.7 | 2010, 2013-2014 | 0 |
| 327 | NA | NA | 0 |
| 361 | NA | NA | 0 |
| 362 | 24.2 | 2013, 2014, 2016 | 0 |
| 560 | 31.0 | 2010-2011, 2014 | 0 |

[a] No prior survey data available.

**Table S2.** Elk trend counts for 8 sampled herds (i.e., herds with Global Positioning System [GPS] location data) located within the Montana designated brucellosis surveillance area (DSA) in southwest Montana, USA, with the 3-year average calf:female ratio, and the years of survey data contributing to the estimate of the average calf:female ratio.

| Herd | Calves:100 females ($c$) | Survey years (calves:100 females) | Sampled count ($s_h$) |
|---|---|---|---|
| Madison Valley | 24.2 | 2013, 2014, 2016 | 3,993 |
| Dome Mountain | 26.0 | 2015-2017 | 3,888 |
| North Madison | 30.0 | 2016[a] | 2,878 |
| Sage Creek | 32.7 | 2010, 2013-2014 | 2,850 |
| Greeley | 31.0 | 2010-2011, 2014 | 1,509 |
| Blacktail | 32.7 | 2010, 2013-2014 | 1,357 |
| Paradise Valley | 35.7 | 2014[a] | 1,222 |
| Mill Creek | 32.0 | 2011[a] | 786 |

[a] No prior survey data available.

**Table S3.** Estimated brucellosis seroprevalence of adult female elk from elk hunting districts within the Montana designated brucellosis surveillance area in southwest Montana, USA, with 95% confidence intervals (CI), the source of the seroprevalence data, and the number of samples (*n*) contributing to the seroprevalence estimate. For brucellosis surveillance project data, seroprevalence values were estimated from samples from hunter-harvested and research-captured elk during 2011-2017, and confidence intervals were calculated from a binomial distribution. For Brennan et al. (2017) data, confidence intervals were derived from models predicting the trend in seroprevalence over time (see Brennan et al. [2017] for additional details).

| Hunting district | Seroprevalence | 95% CI | | Source | *n* |
|---|---|---|---|---|---|
| 317 | 0.53 | 0.36 | 0.70 | Brucellosis surveillance project | 30 |
| 323 | 0.52 | 0.27 | 0.75 | Brennan et al. 2017[a] | 76 |
| 362 | 0.36 | 0.26 | 0.47 | Brennan et al. 2017 | 707 |
| 360 | 0.21 | 0.09 | 0.38 | Brennan et al. 2017 | 225 |
| 313 | 0.20 | 0.13 | 0.31 | Brucellosis surveillance project | 74 |
| 324 | 0.20 | 0.04 | 0.43 | Brennan et al. 2017 | 62 |
| 311 | 0.17 | 0.09 | 0.28 | Brucellosis surveillance project | 60 |
| 310 | 0.12 | 0.01 | 0.42 | Brennan et al. 2017 | 213 |
| 316 | 0.12 | 0.00 | 0.72 | Brennan et al. 2017 | 0 |
| 326 | 0.12 | 0.07 | 0.20 | Brucellosis surveillance project | 100 |
| 301/309 | 0.04[b] | 0.00[b] | 0.24[b] | Brennan et al. 2017 | 10 |
| 361 | 0.08 | 0.01 | 0.26 | Brennan et al. 2017 | 29 |
| 314 | 0.06 | 0.02 | 0.12 | Brennan et al. 2017 | 245 |
| 327 | 0.06 | 0.00 | 0.22 | Brennan et al. 2017 | 20 |
| 325 | 0.05 | 0.02 | 0.12 | Brucellosis surveillance project | 92 |
| 330 | 0.02 | 0.00 | 0.14 | Brennan et al. 2017 | 21 |
| 560 | 0.02 | 0.01 | 0.07 | Brucellosis surveillance project | 106 |

[a] Brennan, A., P. C. Cross, K. Portacci, B. M. Scurlock, and W. H. Edwards. 2017. Shifting brucellosis risk in livestock coincides with spreading seroprevalence in elk. PLoS ONE 12:e0178780.

[b] Seroprevalence estimate for hunting district 301 only.

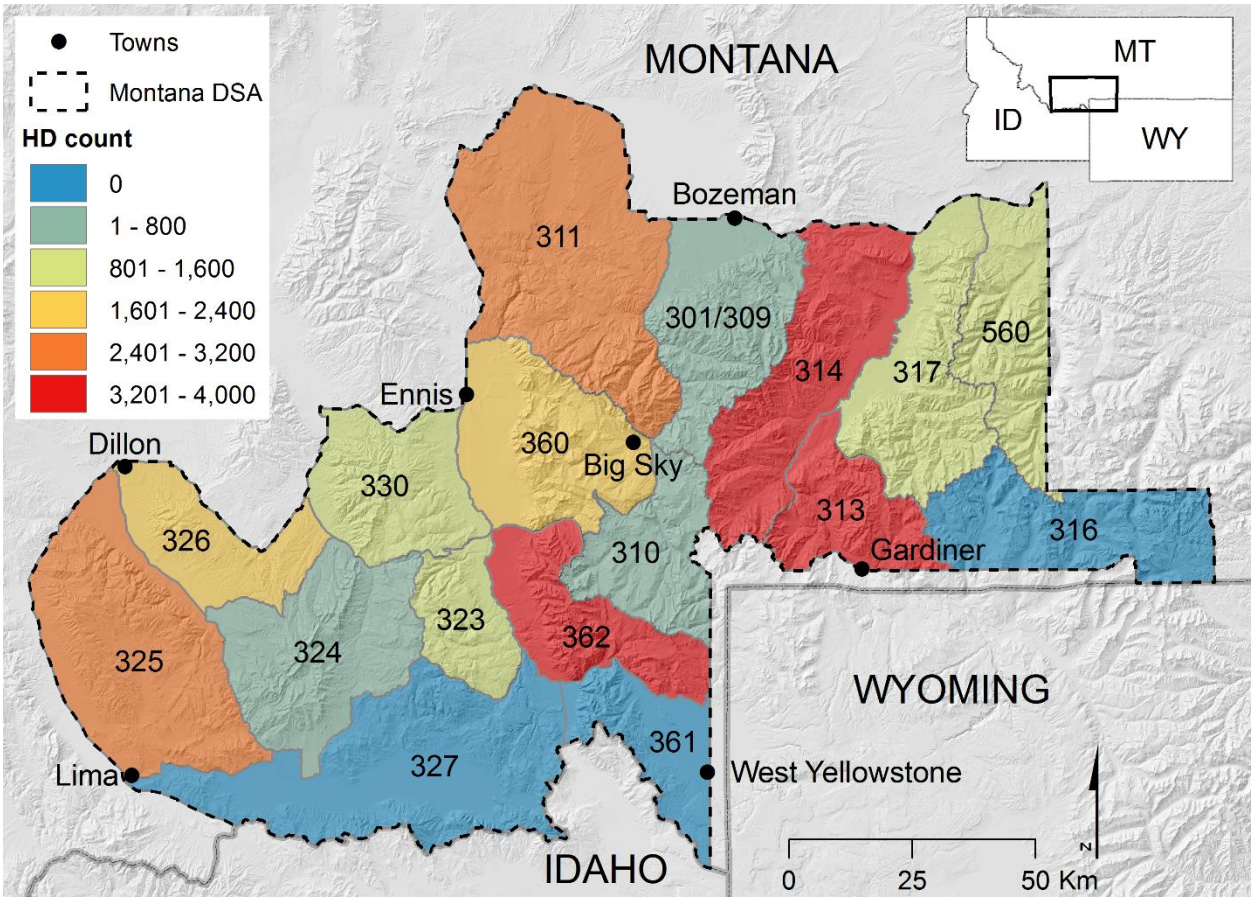


**Figure S1.** Estimated number of total elk during winter located within the portion of elk hunting districts (HD; labeled with black text) that fall within the boundary of the Montana designated brucellosis surveillance area (DSA) in southwest Montana, USA. Shading depicts hillshade of elevation.

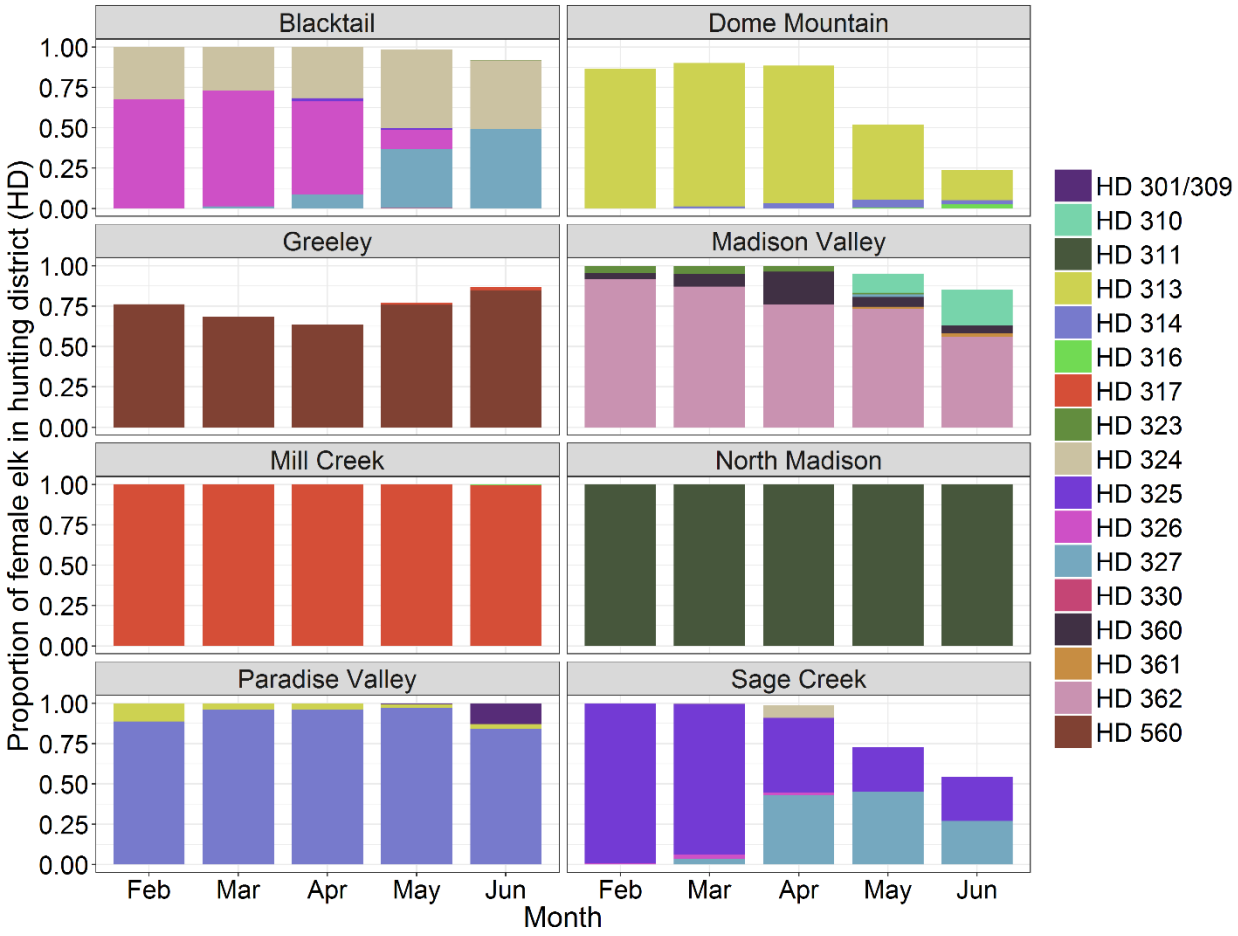


**Figure S2.** Estimated monthly proportion of adult female elk from 8 herds within the portion of elk hunting districts (HD) that were within the boundary of the Montana designated brucellosis surveillance area in southwest Montana, USA. We estimated the time individual collared elk were within the borders of each hunting district in each day, and averaged daily values to estimate monthly proportions. Where total monthly proportions <1, it indicates that a portion of that herd has exited the DSA. Labels above each panel indicate names of elk herds. Note that February proportions are estimated from 15 February forward.

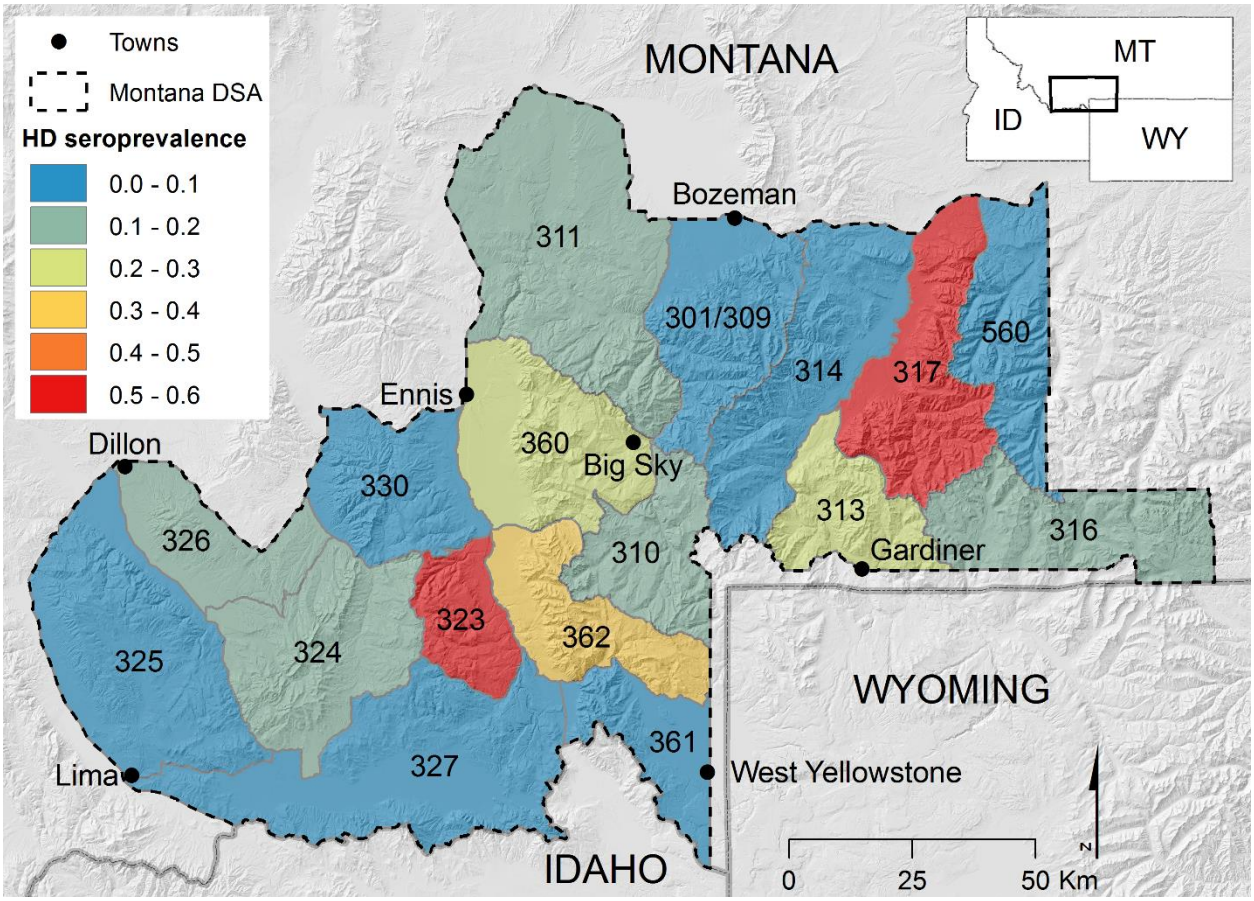


**Figure S3.** Estimated brucellosis seroprevalence of adult female elk located within the portion of elk hunting districts (HD; labeled with black text) that fall within the boundary of the Montana designated brucellosis surveillance area (DSA) in southwest Montana, USA. Shading depicts hillshade of elevation.

**APPENDIX S4.** Areas of livestock grazing during transmission risk period for brucellosis.

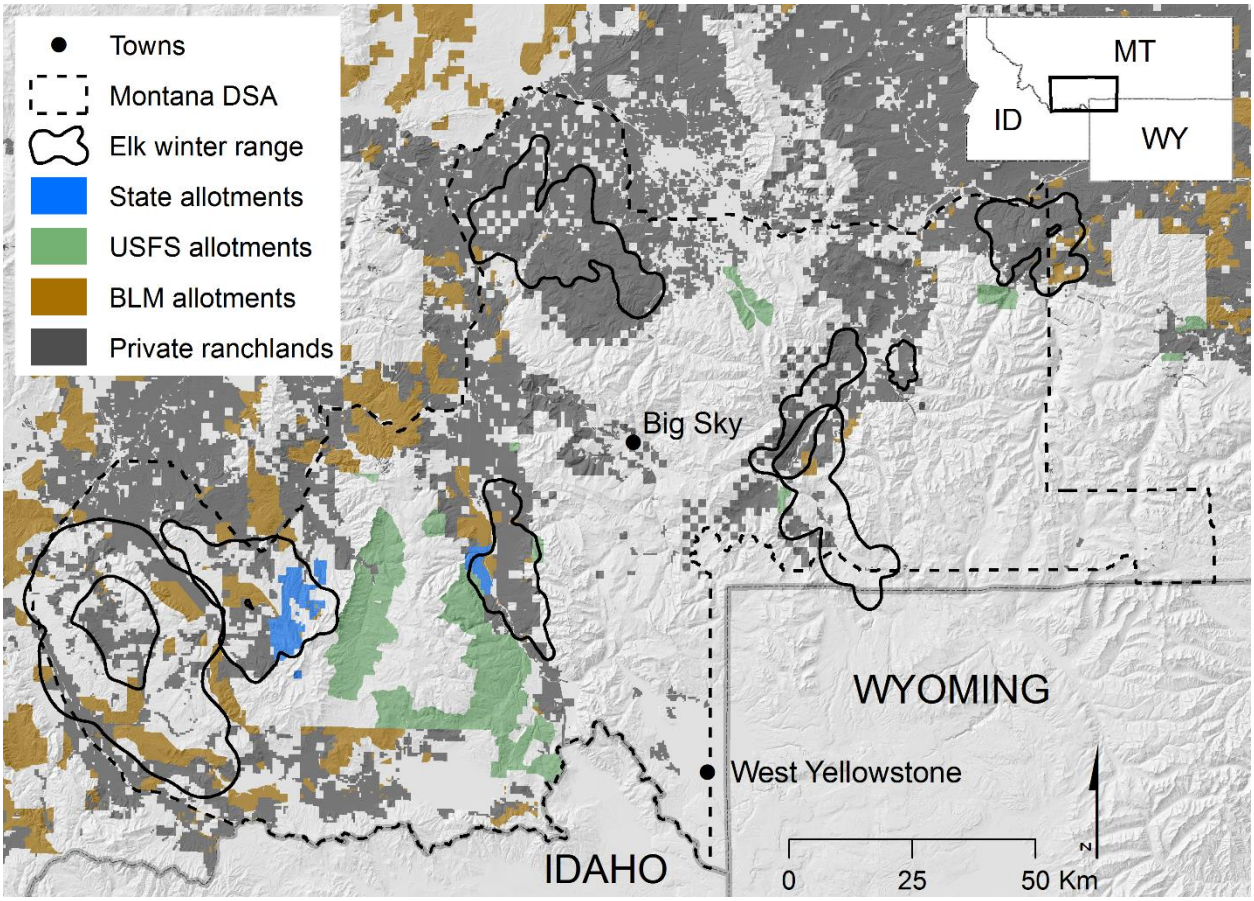


**Figure S1.** Winter ranges of 8 elk herds in southwest Montana, USA, with areas of livestock grazing during the transmission risk period for brucellosis (15 February-30 June). Areas of livestock grazing were defined as state grazing allotments, U.S. Forest Service (USFS) grazing allotments, Bureau of Land Management (BLM) grazing allotments, and private ranchlands in Montana with ≥0.4 hectares of grazing area. Note that only livestock allotments that were stocked with livestock for some portion of the risk period are shown. Shading depicts hillshade of elevation.

**APPENDIX S5.** Results of resource selection functions for adult female elk in southwest Montana, USA during winter, spring, and summer seasons.

**Table S1.** Coefficients (β), standard errors (SE), 95% confidence intervals (CI), and variance estimates of random intercepts from the winter (15 February-31 March) resource selection function estimating the relative probability of occurrence of adult female elk in southwest Montana, USA.

| Variable | β | SE | 95% CI | |
|---|---|---|---|---|
| Elevation | 11.126 | 0.128 | 10.876 | 11.377 |
| Elevation$^2$ | -2.926 | 0.032 | -2.989 | -2.863 |
| Slope | 15.443 | 0.088 | 15.270 | 15.615 |
| Slope$^2$ | -43.678 | 0.277 | -44.221 | -43.135 |
| Terrain position index | 15.353 | 0.162 | 15.035 | 15.671 |
| Solar radiation | -30.181 | 0.255 | -30.680 | -29.682 |
| Solar radiation$^2$ | 21.377 | 0.177 | 21.030 | 21.724 |
| ln(Distance to motorized roads) | 0.638 | 0.007 | 0.623 | 0.653 |
| Forest | -1.807 | 0.019 | -1.844 | -1.771 |
| Shrub | -0.789 | 0.015 | -0.819 | -0.760 |
| Agriculture | 0.760 | 0.032 | 0.699 | 0.822 |
| Snow cover | -0.127 | 0.006 | -0.139 | -0.115 |
| Daily NDVI | 0.853 | 0.043 | 0.770 | 0.937 |
| Daily NDVI$^2$ | -1.226 | 0.058 | -1.341 | -1.112 |
| Annual integrated NDVI | -0.206 | 0.019 | -0.243 | -0.170 |
| Random effects | Variance | | | |
| Elk-year | 0.024 | | | |
| Herd | 0.061 | | | |

**Table S2.** Coefficients (β), standard errors (SE), 95% confidence intervals (CI), and variance estimates of random intercepts from the spring (1 April-31 May) resource selection function estimating the relative probability of occurrence of adult female elk in southwest Montana, USA.

| Variable | β | SE | 95% CI | |
|---|---|---|---|---|
| Elevation | 15.541 | 0.11 | 15.334 | 15.748 |
| Elevation$^2$ | -4.052 | 0.03 | -4.103 | -4.001 |
| Slope | 10.611 | 0.07 | 10.48 | 10.742 |
| Slope$^2$ | -35.573 | 0.21 | -35.98 | -35.17 |
| Terrain position index | 11.046 | 0.11 | 10.822 | 11.271 |
| Solar radiation | -21.415 | 0.35 | -22.09 | -20.74 |
| Solar radiation$^2$ | 16.007 | 0.24 | 15.543 | 16.471 |
| ln(Distance to motorized roads) | 0.443 | 0.01 | 0.4318 | 0.4535 |
| Forest | -0.969 | 0.01 | -0.988 | -0.951 |
| Shrub | 0.090 | 0.01 | 0.0728 | 0.1073 |
| Agriculture | 1.017 | 0.01 | 0.9894 | 1.0451 |
| Snow cover | -0.787 | 0.01 | -0.81 | -0.764 |
| Daily NDVI | 7.693 | 0.04 | 7.6211 | 7.7641 |
| Daily NDVI$^2$ | -6.616 | 0.03 | -6.678 | -6.553 |
| Annual integrated NDVI | 0.778 | 0.02 | 0.7482 | 0.8086 |
| Random effects | Variance | | | |
| Elk-year | 0.062 | | | |
| Herd | 0.027 | | | |

**Table S3.** Coefficients (β), standard errors (SE), 95% confidence intervals (CI), and variance estimates of random intercepts from the summer (1 June-30 June) resource selection function estimating the relative probability of occurrence of adult female elk in southwest Montana, USA.

| Variable | β | SE | 95% CI | |
|---|---|---|---|---|
| Elevation | -0.455 | 0.14 | -0.721 | -0.189 |
| Elevation$^2$ | -0.016 | 0.03 | -0.076 | 0.0447 |
| Slope | 4.993 | 0.09 | 4.8242 | 5.1611 |
| Slope$^2$ | -18.735 | 0.23 | -19.19 | -18.28 |
| Terrain position index | 6.014 | 0.12 | 5.7723 | 6.2561 |
| Solar radiation | -8.618 | 0.35 | -9.304 | -7.932 |
| Solar radiation$^2$ | 7.194 | 0.24 | 6.731 | 7.6579 |
| ln(Distance to motorized roads) | 0.251 | 0.01 | 0.237 | 0.2659 |
| Forest | 0.165 | 0.01 | 0.1393 | 0.1912 |
| Shrub | 1.054 | 0.01 | 1.0289 | 1.0793 |
| Agriculture | 1.203 | 0.03 | 1.1469 | 1.2598 |
| Snow cover | -0.319 | 0.06 | -0.441 | -0.197 |
| Daily NDVI | 10.231 | 0.13 | 9.9799 | 10.482 |
| Daily NDVI$^2$ | -6.057 | 0.09 | -6.229 | -5.884 |
| Annual integrated NDVI | 0.033 | 0.03 | -0.016 | 0.0825 |
| Random effects | Variance | | | |
| Elk-year | 0.070 | | | |
| Herd | 0.007 | | | |

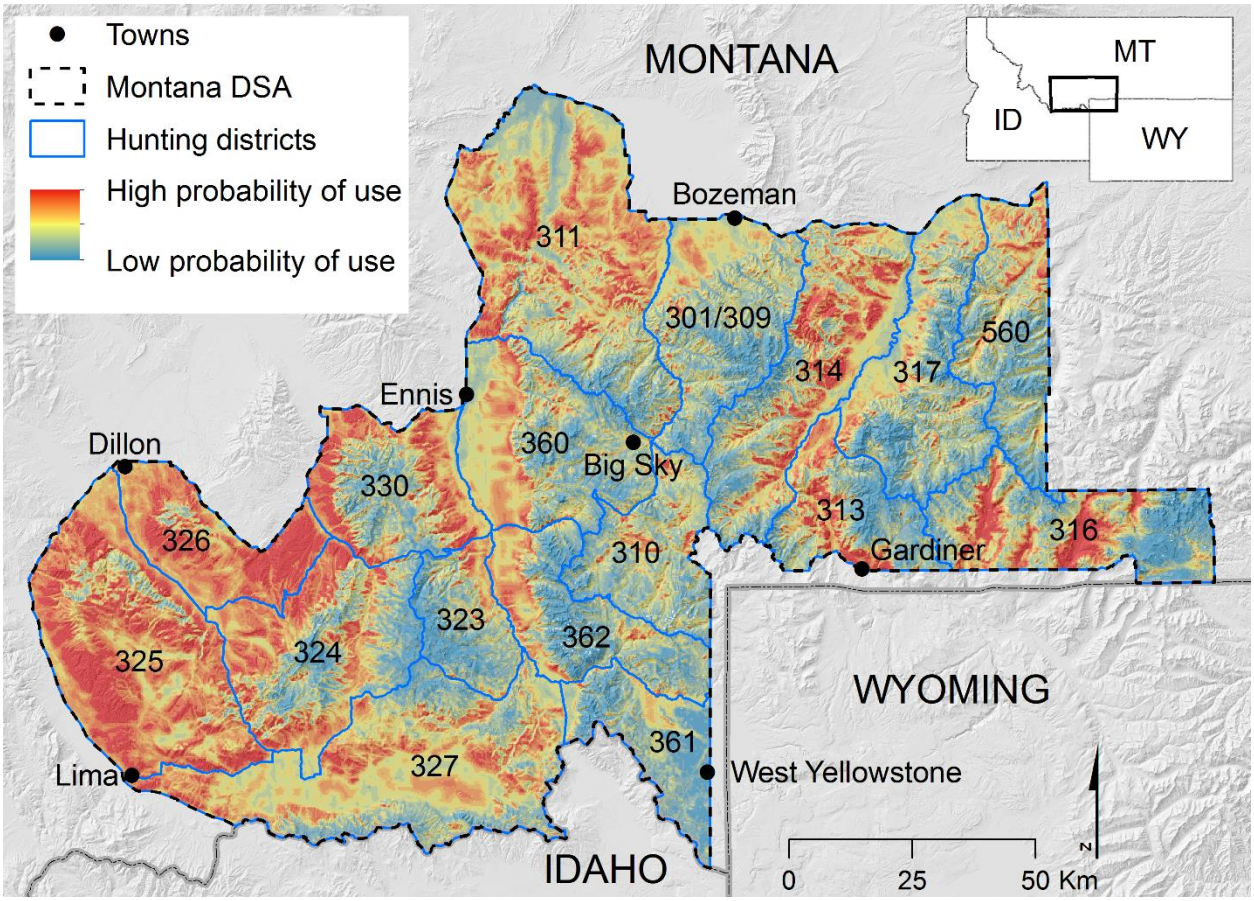


**Figure S1.** Predicted relative probability of use by adult female elk during February (15 February-28 February) within the portion of elk hunting districts (HDs; labeled with black text) that fall within the boundary of the Montana designated brucellosis surveillance area (DSA) in southwest Montana, USA. The monthly estimate was produced by summing estimates of the daily relative probability of use during all days of the month. Note that HD 301 and HD 309 were merged in our analyses (see Methods), and the portion of HDs 301/309, 311, 316, and 560 that extend beyond the border of the DSA are not shown. Shading depicts hillshade of elevation.

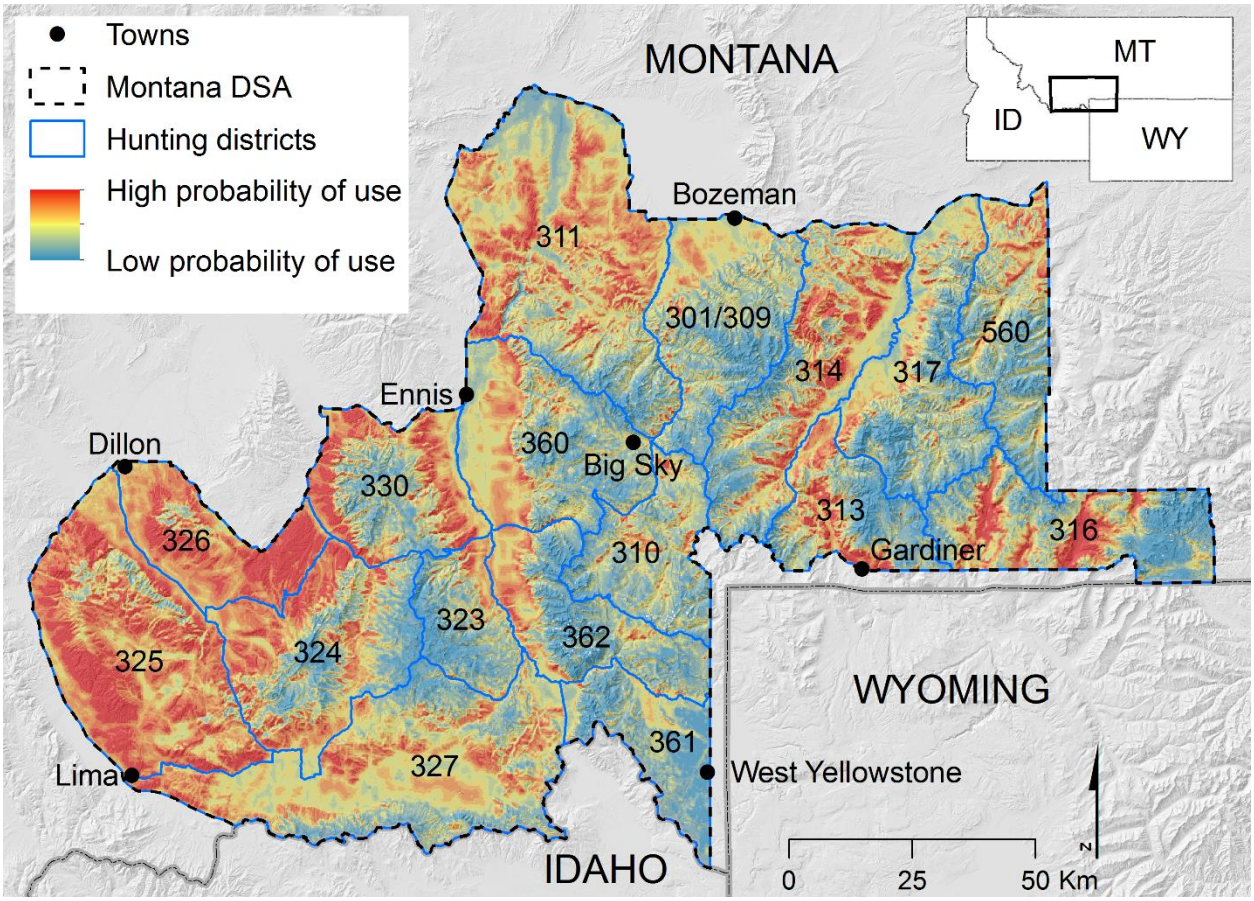


**Figure S2.** Predicted relative probability of use by adult female elk during March within the portion of elk hunting districts (HDs; labeled with black text) that fall within the boundary of the Montana designated brucellosis surveillance area (DSA) in southwest Montana, USA. The monthly estimate was produced by summing estimates of the daily relative probability of use during all days of the month. Note that HD 301 and HD 309 were merged in our analyses (see Methods), and the portion of HDs 301/309, 311, 316, and 560 that extend beyond the border of the DSA are not shown. Shading depicts hillshade of elevation.

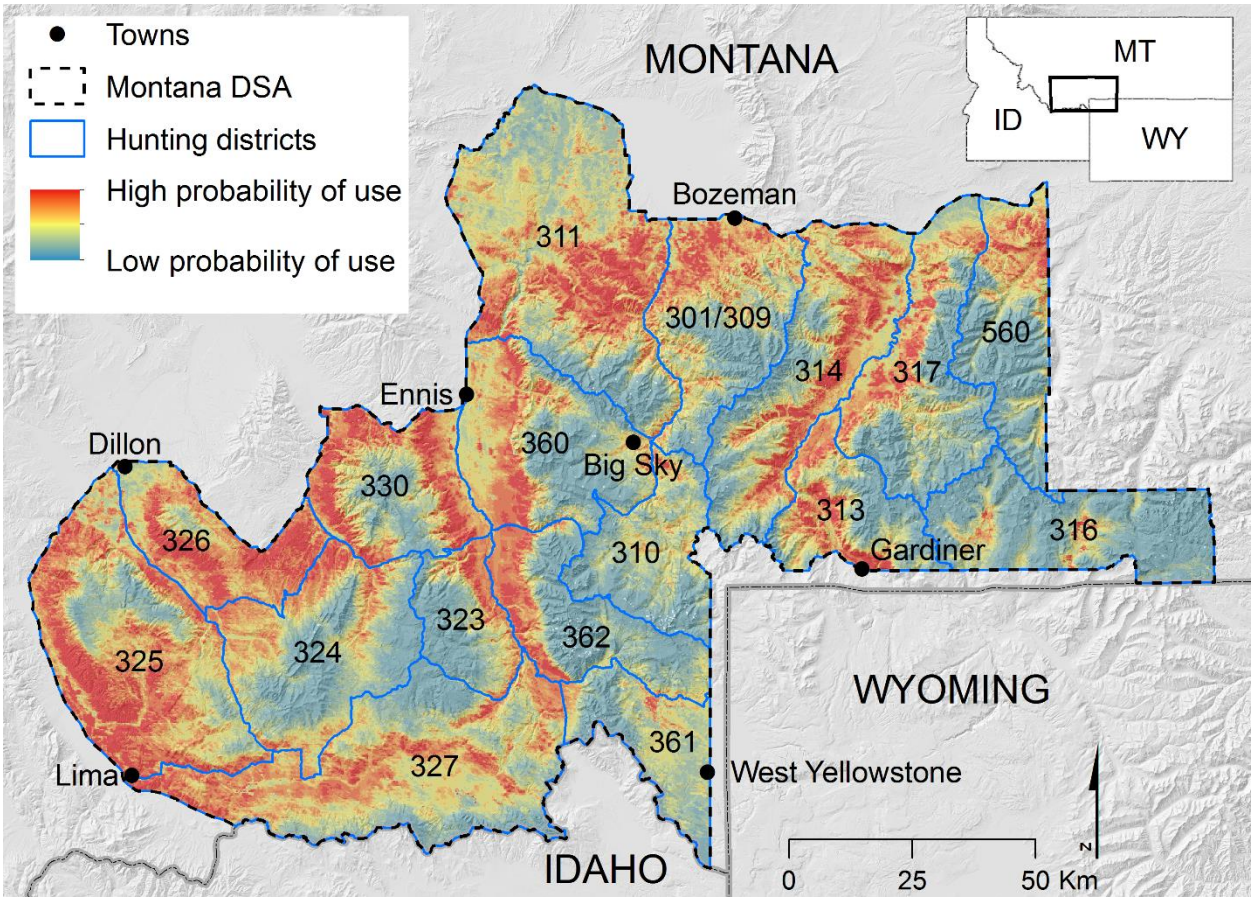


**Figure S3.** Predicted relative probability of use by adult female elk during April within the portion of elk hunting districts (HDs; labeled with black text) that fall within the boundary of the Montana designated brucellosis surveillance area (DSA) in southwest Montana, USA. The monthly estimate was produced by summing estimates of the daily relative probability of use during all days of the month. Note that HD 301 and HD 309 were merged in our analyses (see Methods), and the portion of HDs 301/309, 311, 316, and 560 that extend beyond the border of the DSA are not shown. Shading depicts hillshade of elevation.

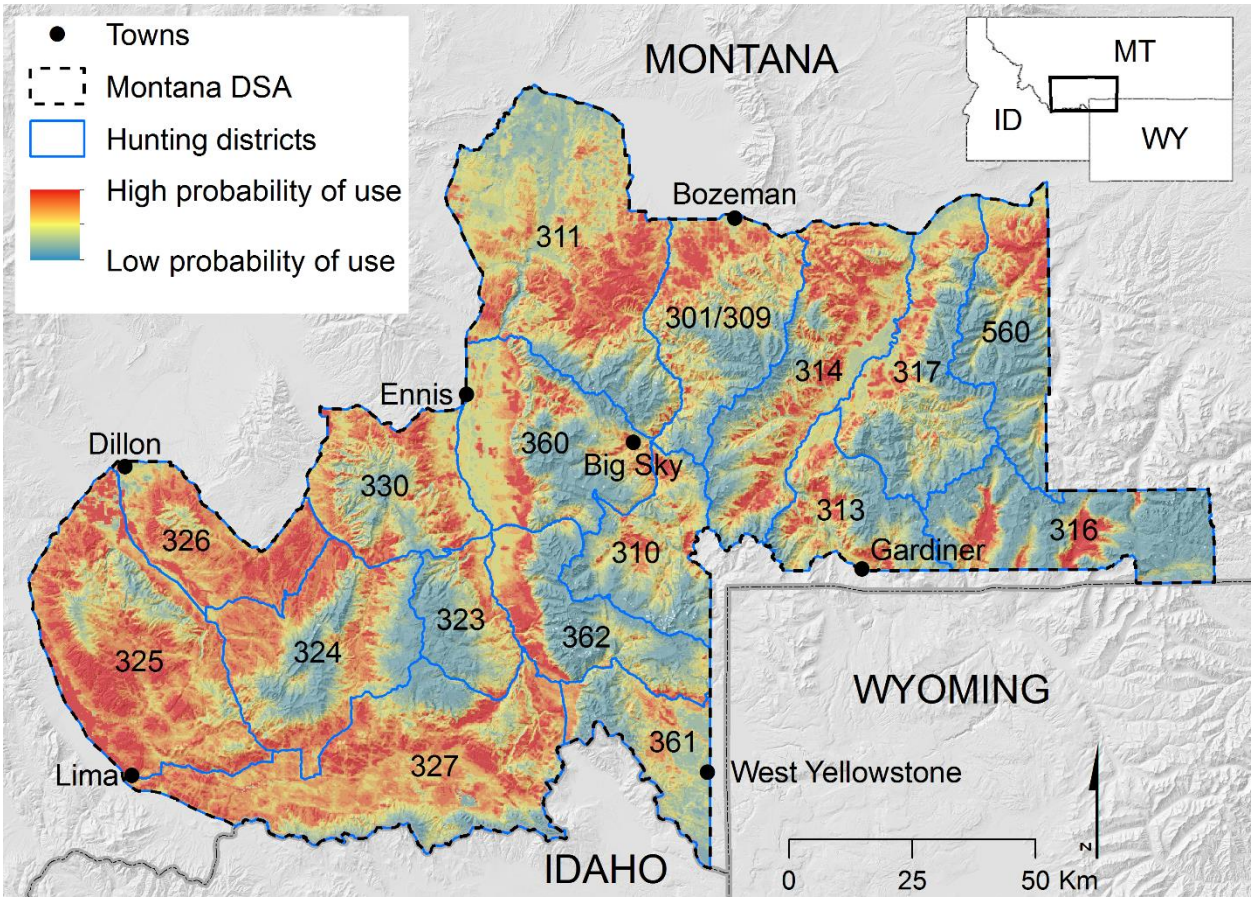


**Figure S4.** Predicted relative probability of use by adult female elk during May within the portion of elk hunting districts (HDs; labeled with black text) that fall within the boundary of the Montana designated brucellosis surveillance area (DSA) in southwest Montana, USA. The monthly estimate was produced by summing estimates of the daily relative probability of use during all days of the month. Note that HD 301 and HD 309 were merged in our analyses (see Methods), and the portion of HDs 301/309, 311, 316, and 560 that extend beyond the border of the DSA are not shown. Shading depicts hillshade of elevation.

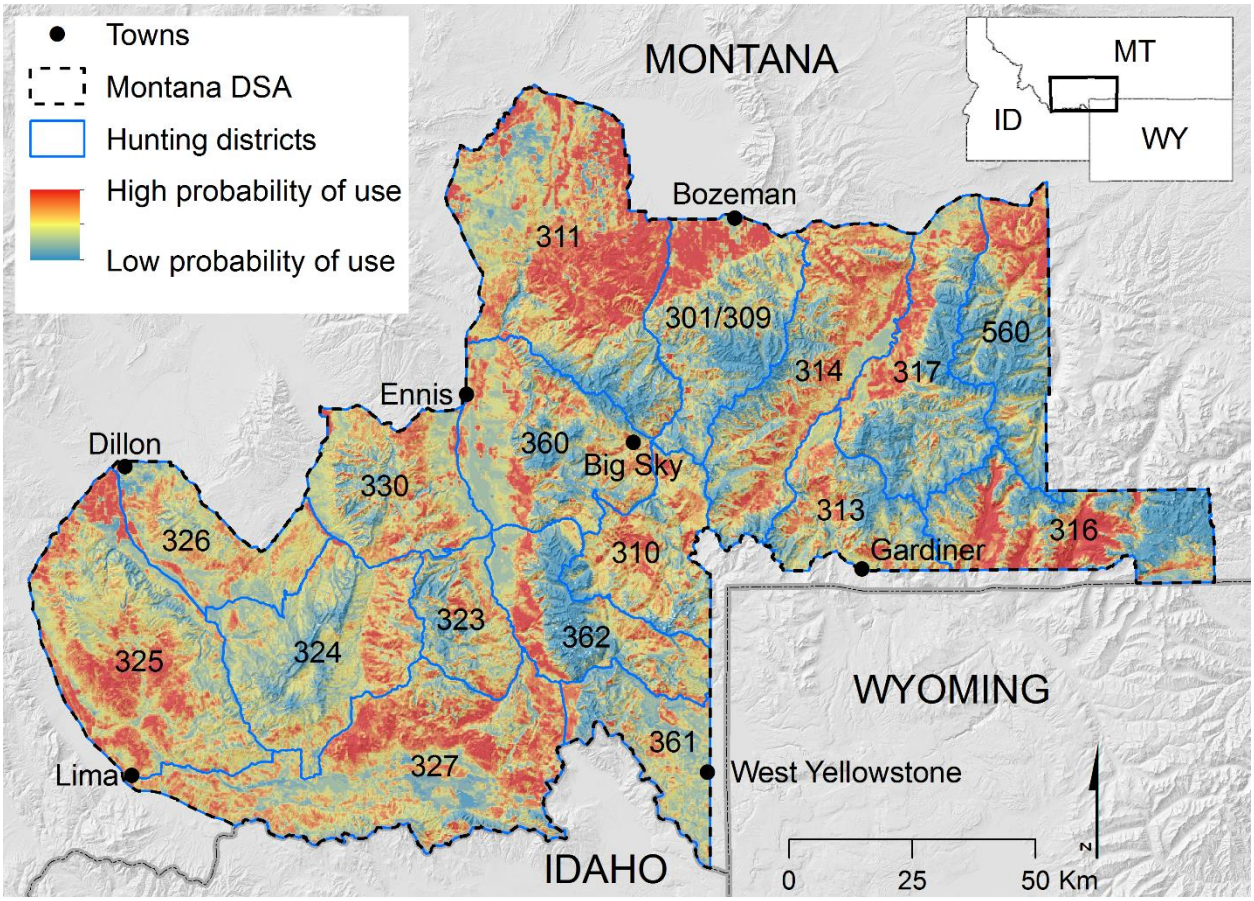


**Figure S5.** Predicted relative probability of use by adult female elk during June within the portion of elk hunting districts (HDs; labeled with black text) that fall within the boundary of the Montana designated brucellosis surveillance area (DSA) in southwest Montana, USA. The monthly estimate was produced by summing estimates of the daily relative probability of use during all days of the month. Note that HD 301 and HD 309 were merged in our analyses (see Methods), and the portion of HDs 301/309, 311, 316, and 560 that extend beyond the border of the DSA are not shown. Shading depicts hillshade of elevation.

**APPENDIX S6.** Results of cross-validation procedure to assess external applicability of resource selection models.

We used a cross-validation procedure to assess the generalizability of our space-use predictions to unsampled elk herds within the Montana designated brucellosis surveillance area. We iteratively fit seasonal resource selection functions (RSFs) using data from 7 of 8 sampled herds (3 seasons × 8 herds = 24 partial RSF models). For each partial RSF, we reclassified the available locations of the excluded herd into 10 ordinal bins based on the percentile range of the partial RSF-predicted scores for those locations. We then calculated the Spearman rank correlation ($r_s$) between the frequency of occurrence of RSF-predicted scores for used locations from the excluded herd and the ranked RSF-availability bins (Fig. S1). This allowed us to evaluate the ability of the partial RSF to predict the space use of the excluded herd.

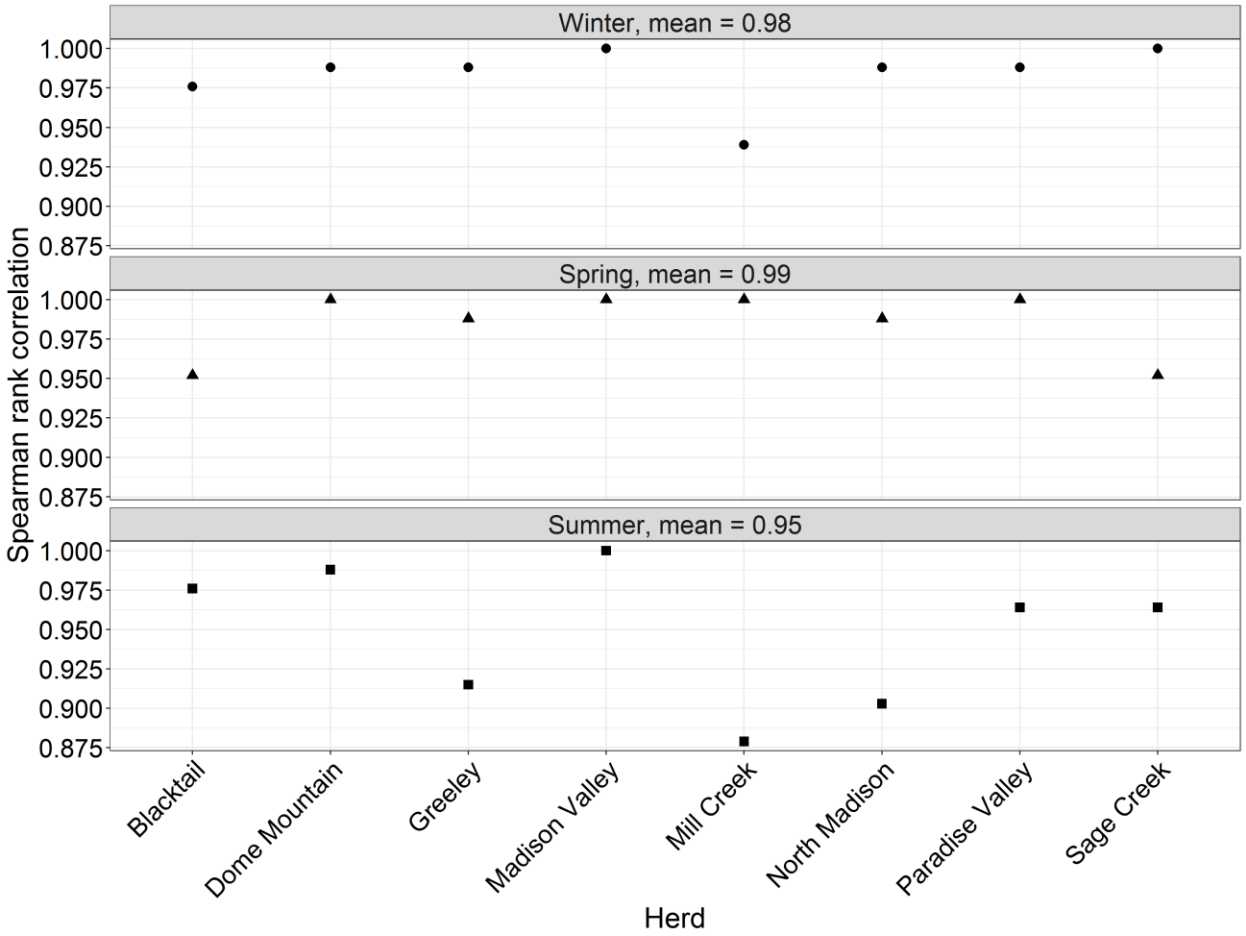


**Figure S1.** Spearman rank correlation ($r_s$) scores for partial RSF models (estimated using data from 7 of 8 sampled herds) built to assess the ability of the model to predict the space use of the excluded herd. The x-axis labels indicate the identity of the herd that was excluded from the partial RSF model.

**APPENDIX S7.** Monthly maps of the predicted risk of brucellosis-induced abortion events by adult female elk.

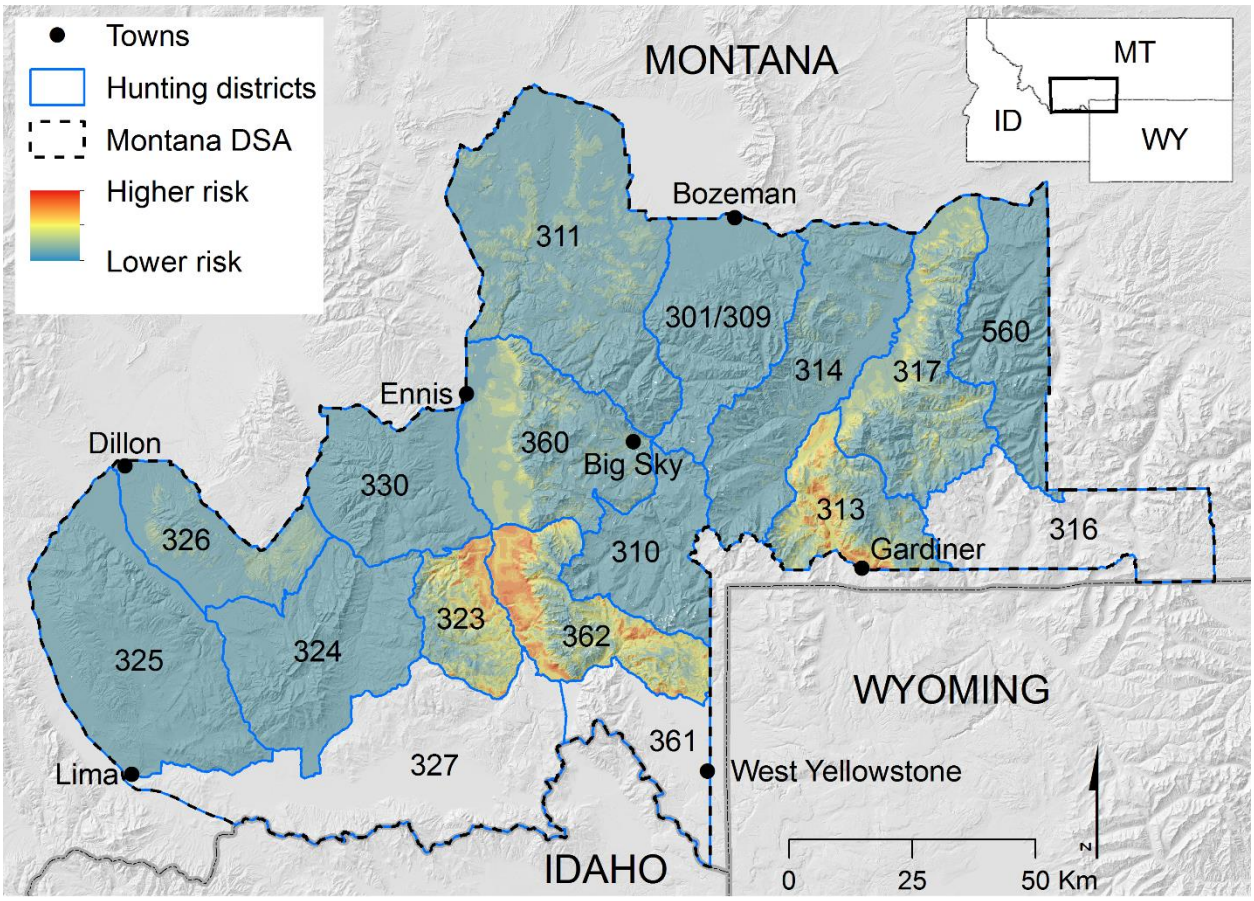


**Figure S1.** Predicted risk of brucellosis-induced abortion events by adult female elk during February (15 February-28 February) within the portion of elk hunting districts (HDs; labeled with black text) that fall within the boundary of the Montana designated brucellosis surveillance area (DSA) in southwest Montana, USA. The monthly estimate was produced by summing estimates of the daily risk of abortion events from 15 February-28 February. Note that HD 301 and HD 309 were merged in our analyses (see Methods), and the portion of HDs 301/309, 311, 316, and 560 that extend beyond the border of the DSA are not shown. Shading depicts hillshade of elevation.

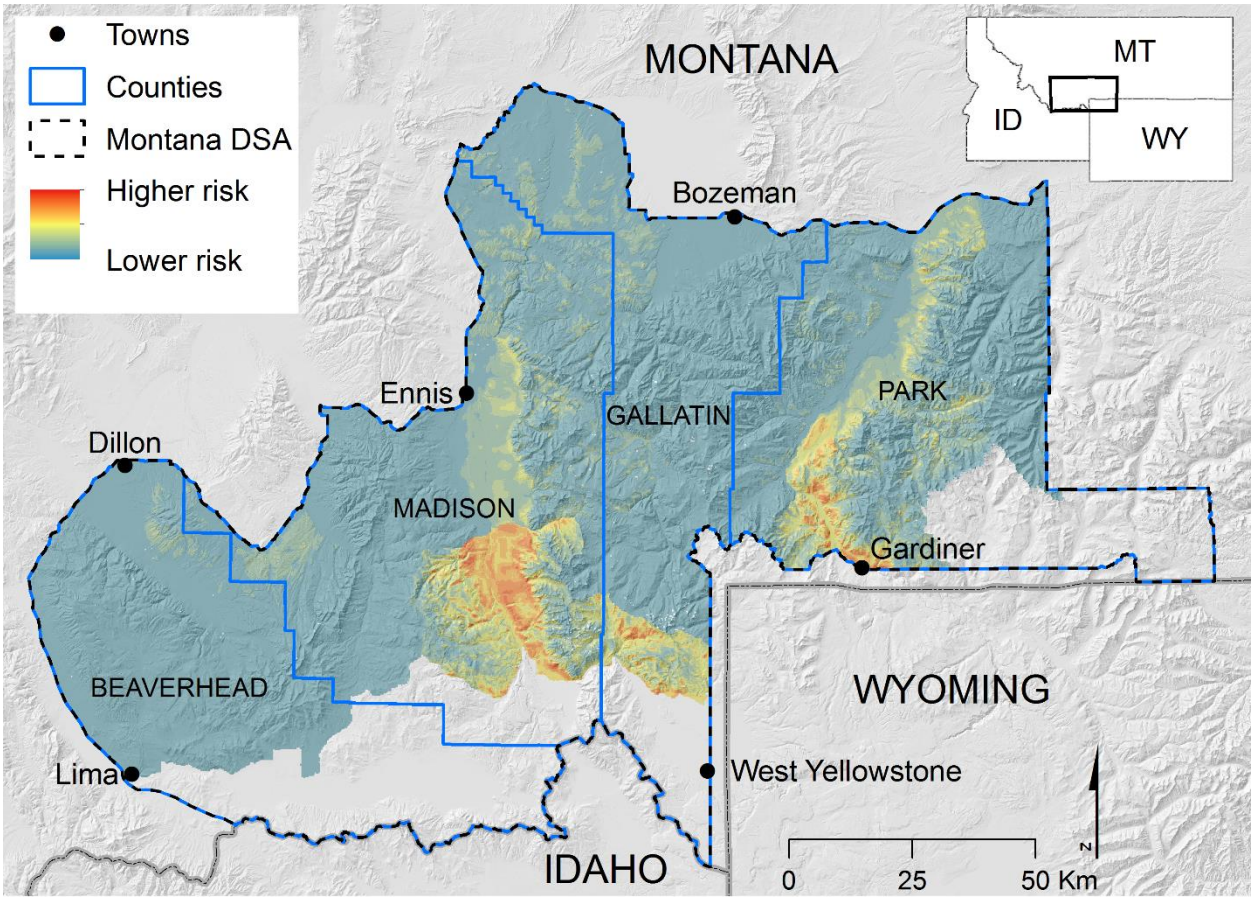


**Figure S2.** Predicted risk of brucellosis-induced abortion events by adult female elk during February (15 February-28 February) within the portion of Montana counties (blue outlines; labeled with black text) that fall within the boundary of the Montana designated brucellosis surveillance area (DSA) in southwest Montana, USA. The monthly estimate was produced by summing estimates of the daily risk of abortion events from 15 February-28 February. Note that portions of the counties that extend beyond the border of the DSA are not shown. Shading depicts hillshade of elevation.

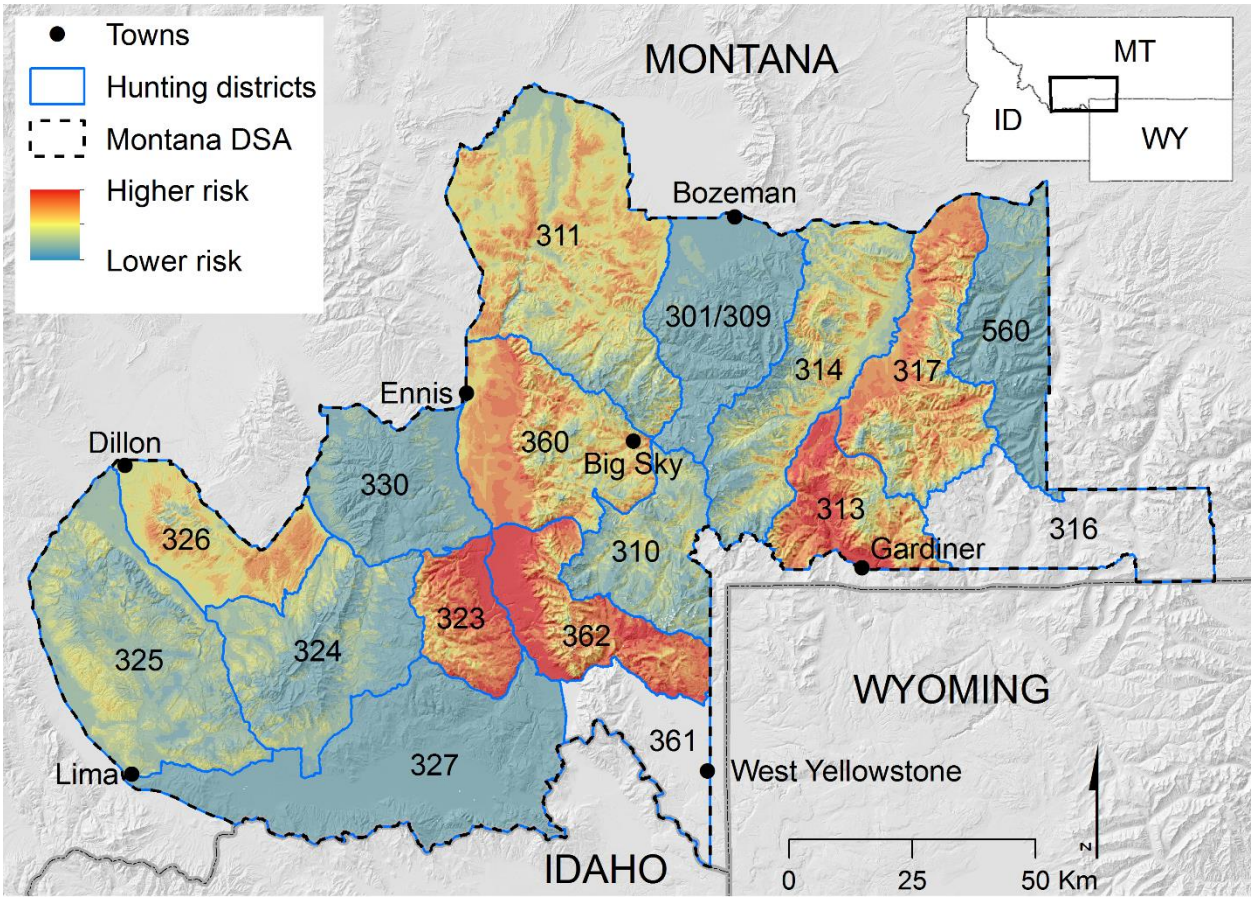


**Figure S3.** Predicted risk of brucellosis-induced abortion events by adult female elk during March within the portion of elk hunting districts (HDs; labeled with black text) that fall within the boundary of the Montana designated brucellosis surveillance area (DSA) in southwest Montana, USA. The monthly estimate was produced by summing estimates of the daily risk of abortion events during all days of the month. Note that HD 301 and HD 309 were merged in our analyses (see Methods), and the portion of HDs 301/309, 311, 316, and 560 that extend beyond the border of the DSA are not shown. Shading depicts hillshade of elevation.

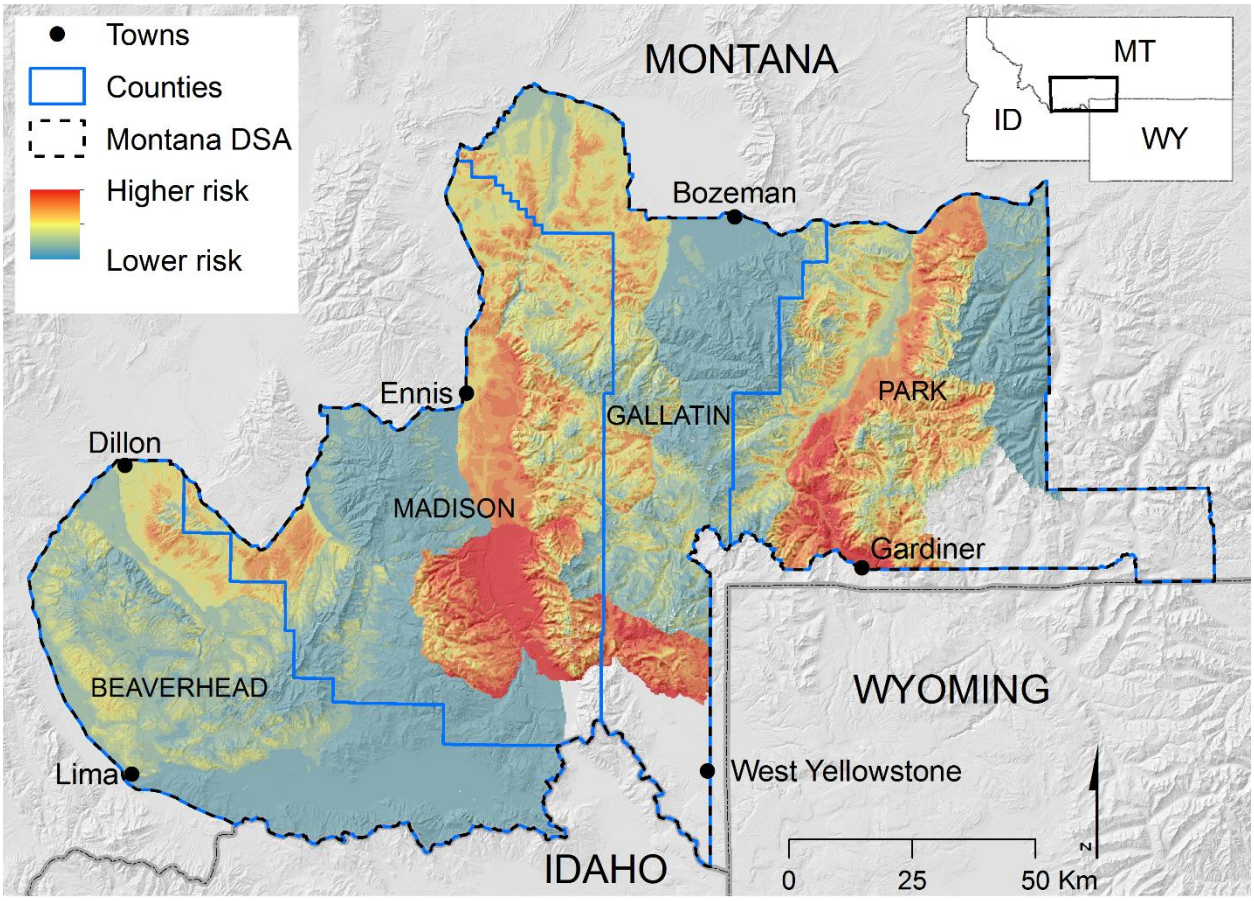


**Figure S4.** Predicted risk of brucellosis-induced abortion events by adult female elk during March within the portion of Montana counties (blue outlines; labeled with black text) that fall within the boundary of the Montana designated brucellosis surveillance area (DSA) in southwest Montana, USA. The monthly estimate was produced by summing estimates of the daily risk of abortion events during all days of the month. Note that portions of the counties that extend beyond the border of the DSA are not shown. Shading depicts hillshade of elevation.

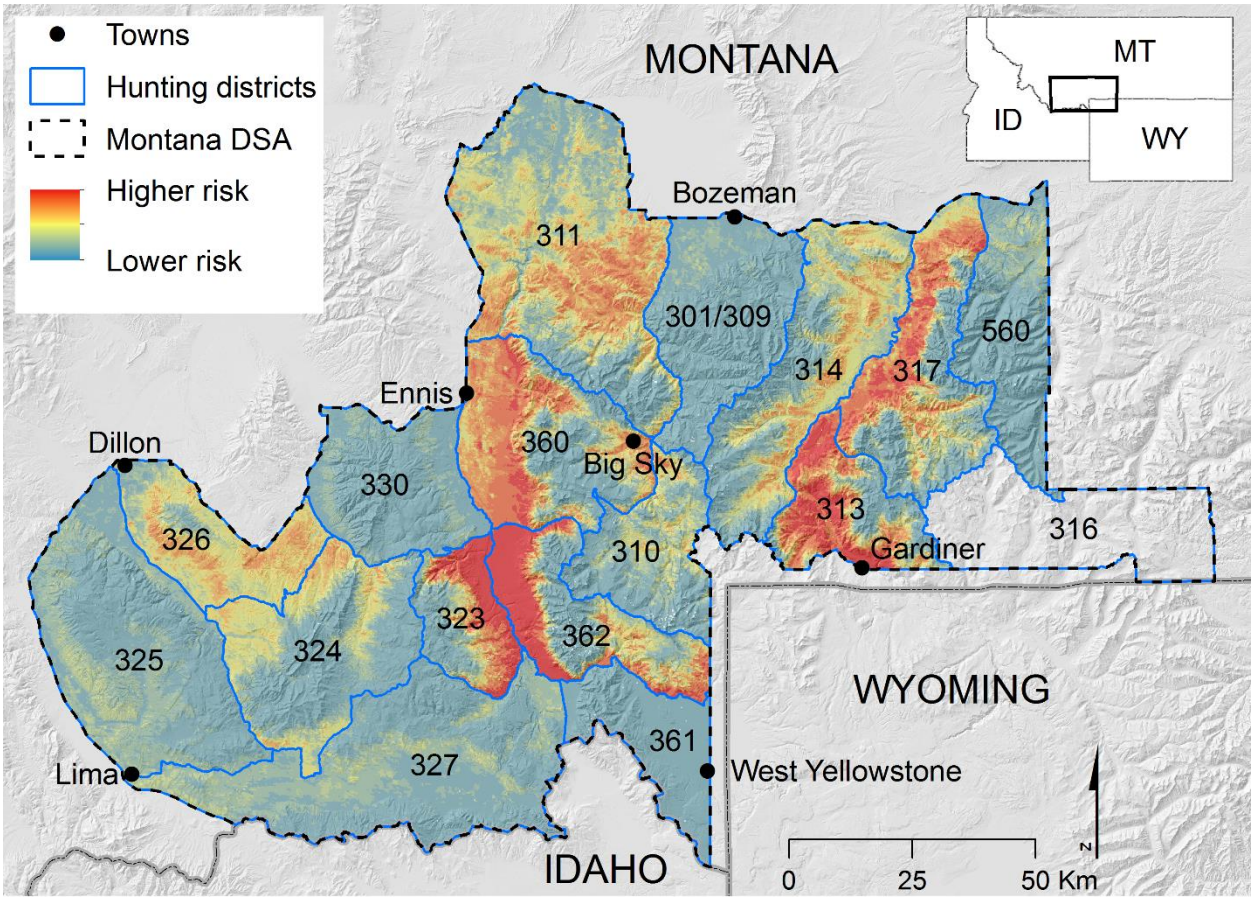


**Figure S5.** Predicted risk of brucellosis-induced abortion events by adult female elk during April within the portion of elk hunting districts (HDs; labeled with black text) that fall within the boundary of the Montana designated brucellosis surveillance area (DSA) in southwest Montana, USA. The monthly estimate was produced by summing estimates of the daily risk of abortion events during all days of the month. Note that HD 301 and HD 309 were merged in our analyses (see Methods), and the portion of HDs 301/309, 311, 316, and 560 that extend beyond the border of the DSA are not shown. Shading depicts hillshade of elevation.

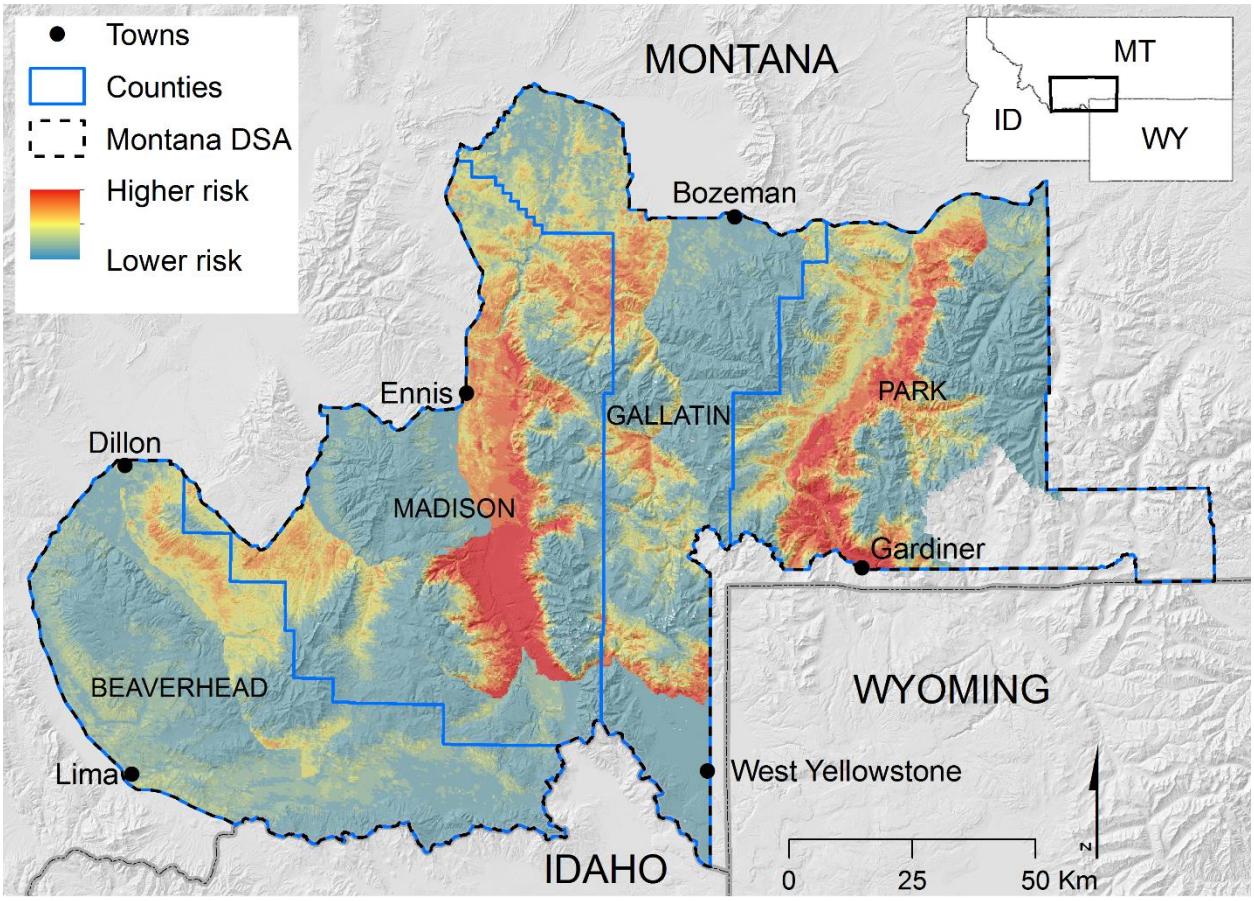


**Figure S6.** Predicted risk of brucellosis-induced abortion events by adult female elk during April within the portion of Montana counties (blue outlines; labeled with black text) that fall within the boundary of the Montana designated brucellosis surveillance area (DSA) in southwest Montana, USA. The monthly estimate was produced by summing estimates of the daily risk of abortion events during all days of the month. Note that portions of the counties that extend beyond the border of the DSA are not shown. Shading depicts hillshade of elevation.

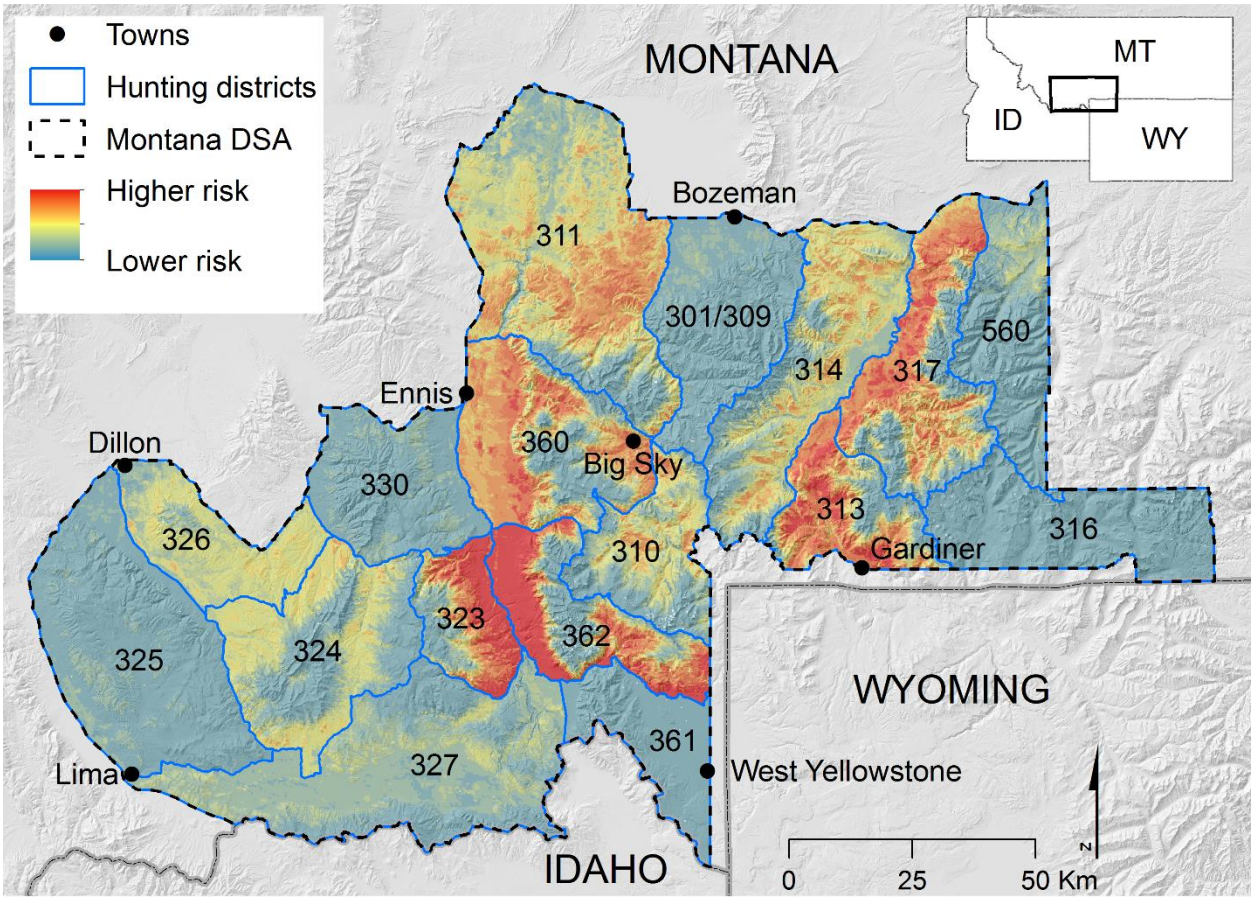


**Figure S7.** Predicted risk of brucellosis-induced abortion events by adult female elk during May within the portion of elk hunting districts (HDs; labeled with black text) that fall within the boundary of the Montana designated brucellosis surveillance area (DSA) in southwest Montana, USA. The monthly estimate was produced by summing estimates of the daily risk of abortion events during all days of the month. Note that HD 301 and HD 309 were merged in our analyses (see Methods), and the portion of HDs 301/309, 311, 316, and 560 that extend beyond the border of the DSA are not shown. Shading depicts hillshade of elevation.

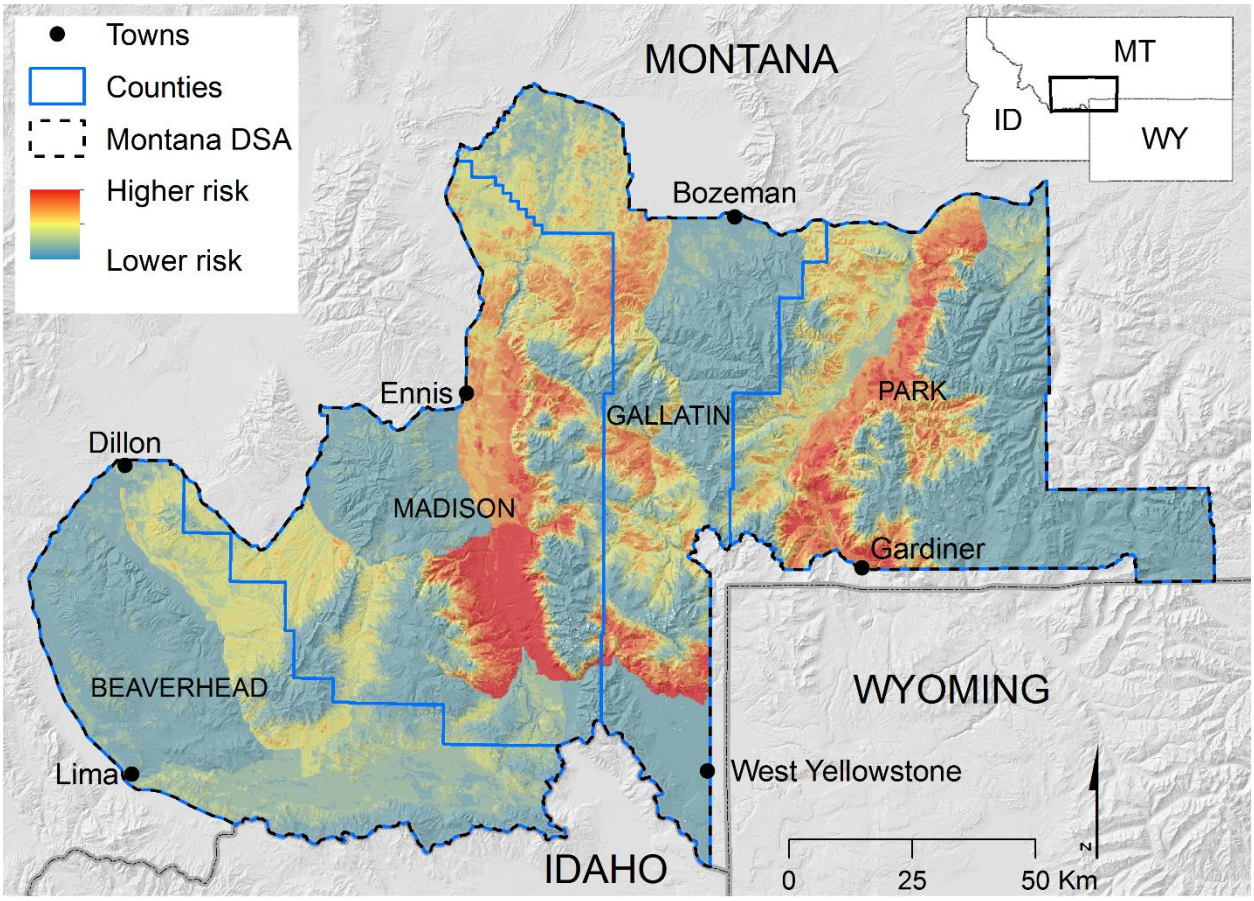


**Figure S8.** Predicted risk of brucellosis-induced abortion events by adult female elk during May within the portion of Montana counties (blue outlines; labeled with black text) that fall within the boundary of the Montana designated brucellosis surveillance area (DSA) in southwest Montana, USA. The monthly estimate was produced by summing estimates of the daily risk of abortion events during all days of the month. Note that portions of the counties that extend beyond the border of the DSA are not shown. Shading depicts hillshade of elevation.

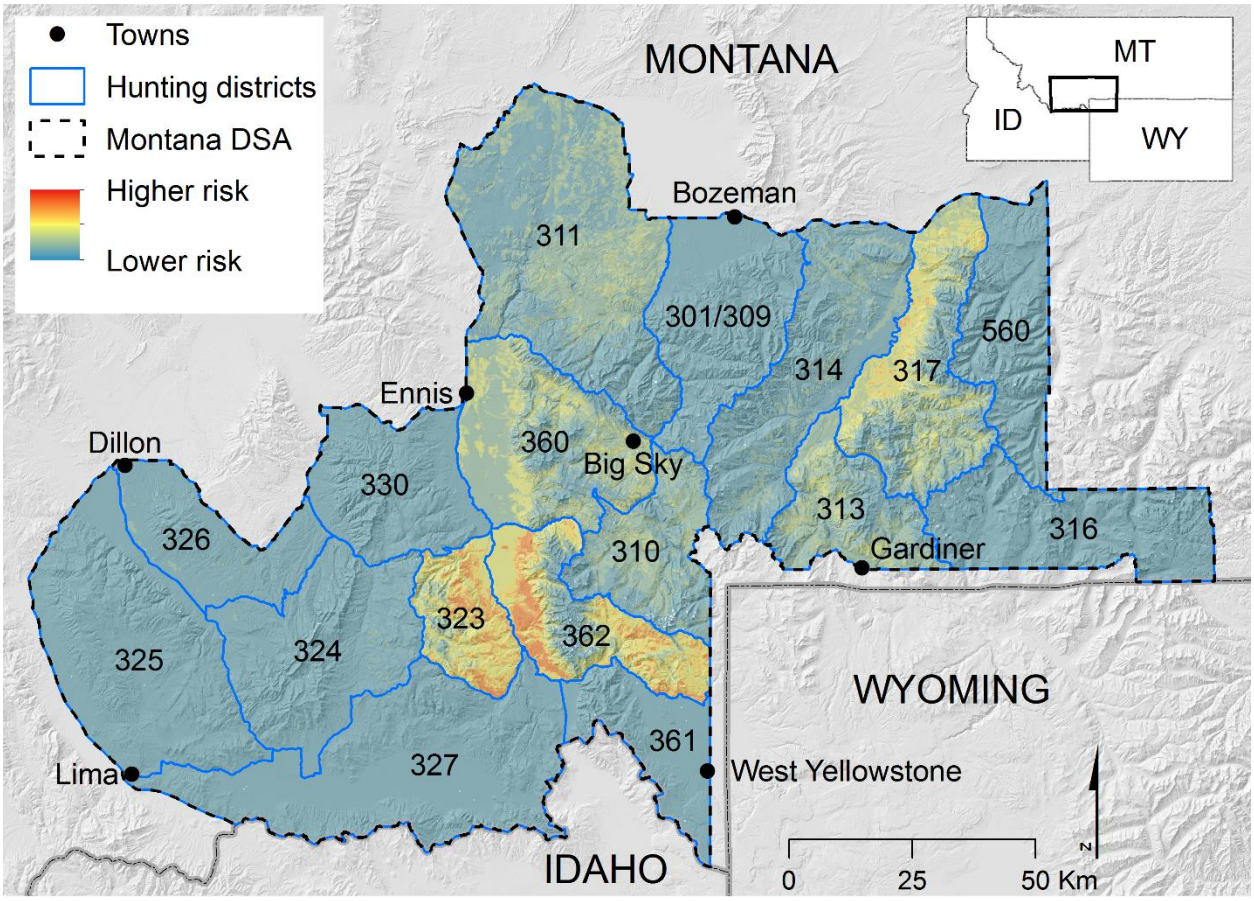


**Figure S9.** Predicted risk of brucellosis-induced abortion events by adult female elk during June within the portion of elk hunting districts (HDs; labeled with black text) that fall within the boundary of the Montana designated brucellosis surveillance area (DSA) in southwest Montana, USA. The monthly estimate was produced by summing estimates of the daily risk of abortion events during all days of the month. Note that HD 301 and HD 309 were merged in our analyses (see Methods), and the portion of HDs 301/309, 311, 316, and 560 that extend beyond the border of the DSA are not shown. Shading depicts hillshade of elevation.

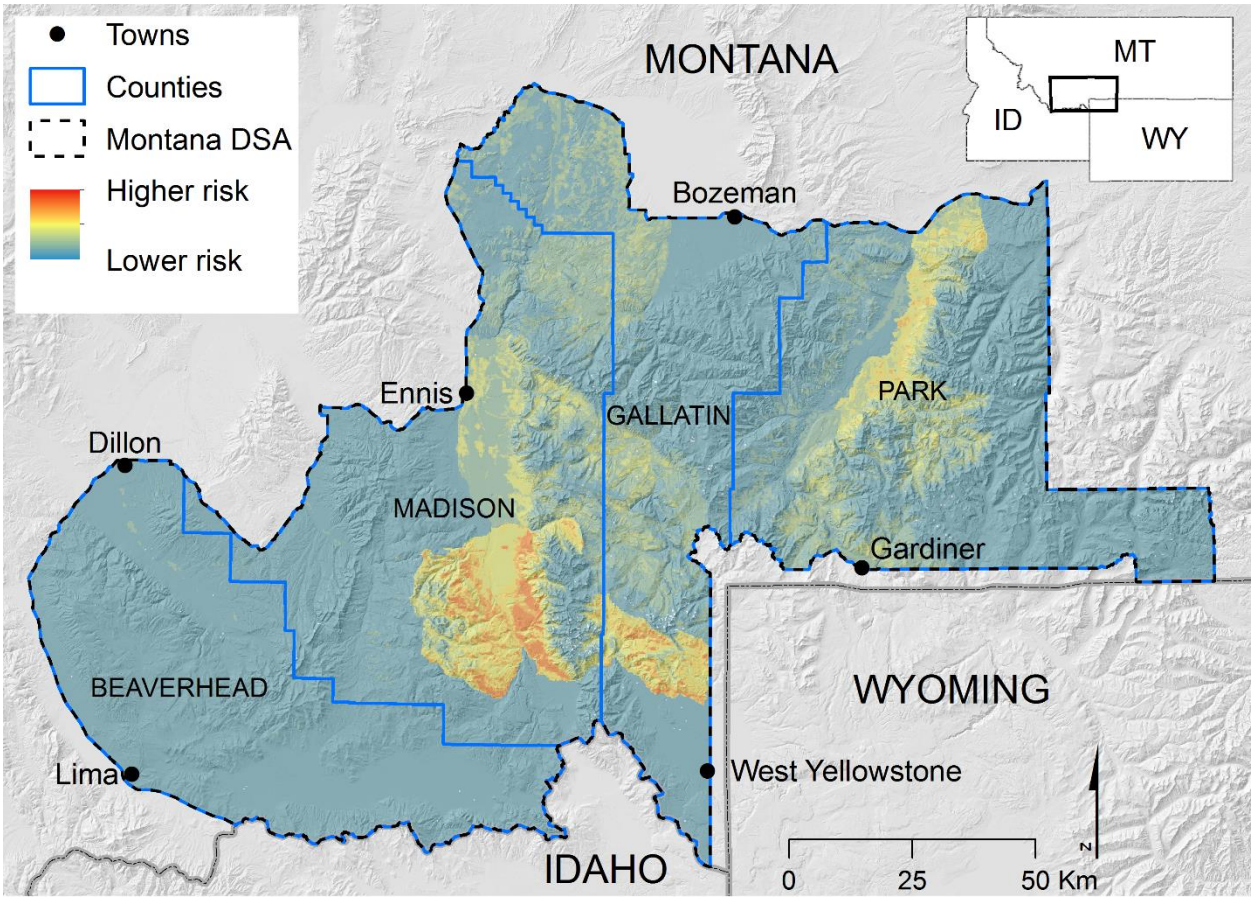


**Figure S10.** Predicted risk of brucellosis-induced abortion events by adult female elk during June within the portion of Montana counties (blue outlines; labeled with black text) that fall within the boundary of the Montana designated brucellosis surveillance area (DSA) in southwest Montana, USA. The monthly estimate was produced by summing estimates of the daily risk of abortion events during all days of the month. Note that portions of the counties that extend beyond the border of the DSA are not shown. Shading depicts hillshade of elevation.

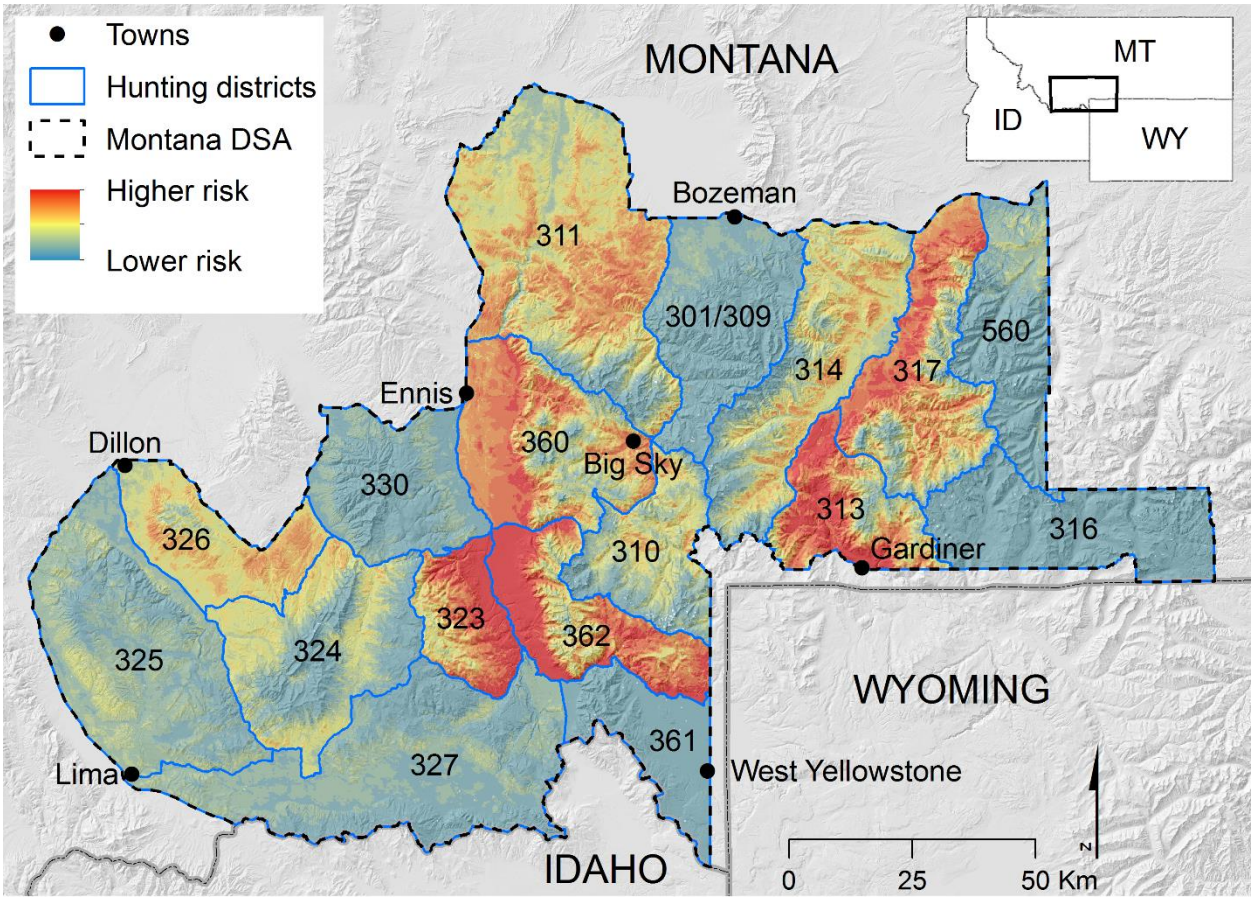


**Figure S11.** Predicted risk of brucellosis-induced abortion events by adult female elk during the risk period for brucellosis transmission (15 February-30 June) within the portion of elk hunting districts (HDs; labeled with black text) that fall within the boundary of the Montana designated brucellosis surveillance area (DSA) in southwest Montana, USA. The estimate was produced by summing estimates of the daily risk of abortion events during all days of the risk period. Note that HD 301 and HD 309 were merged in our analyses (see Methods), and the portion of HDs 301/309, 311, 316, and 560 that extend beyond the border of the DSA are not shown. Shading depicts hillshade of elevation.

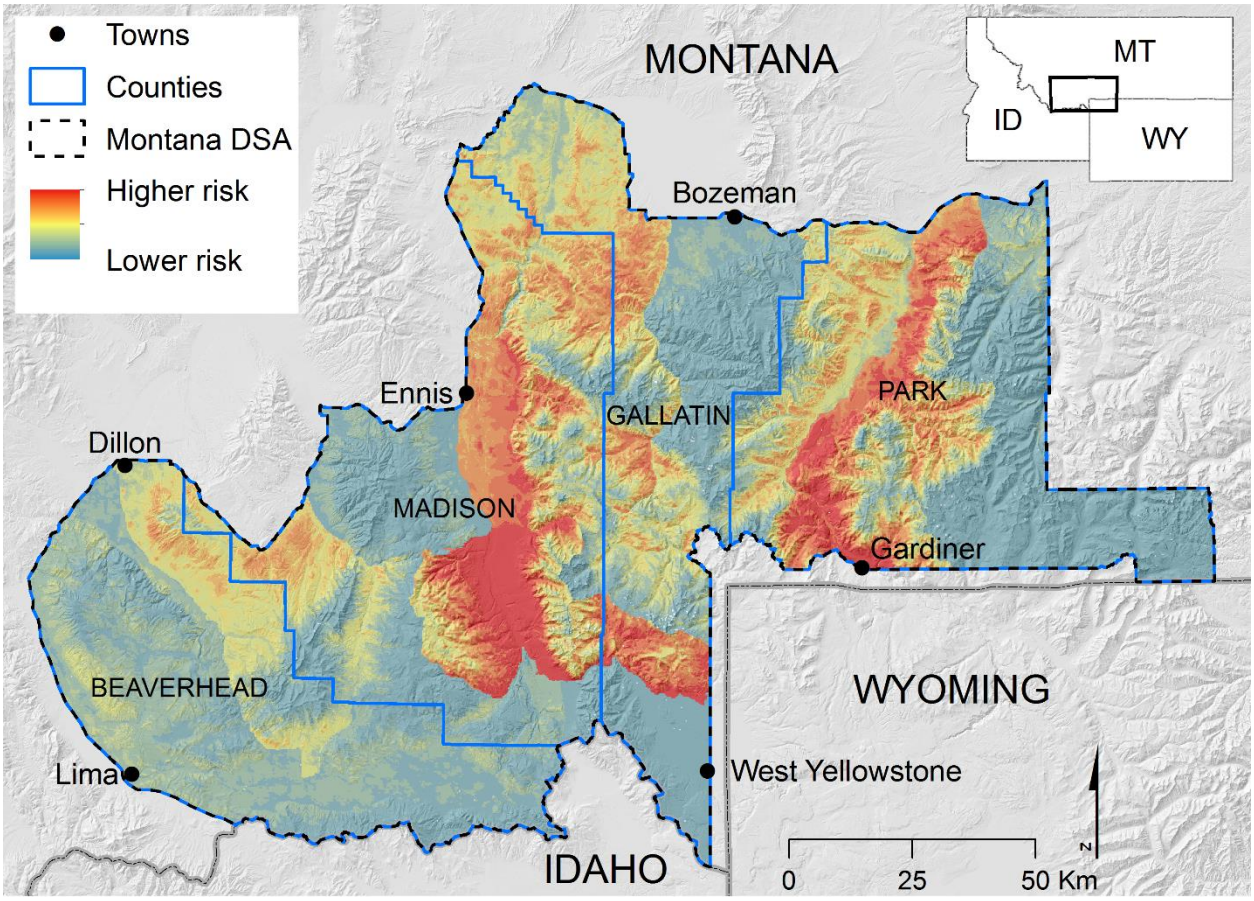


**Figure S12.** Predicted risk of brucellosis-induced abortion events by adult female elk during the risk period for brucellosis transmission (15 February-30 June) within the portion of Montana counties (blue outlines; labeled with black text) that fall within the boundary of the Montana designated brucellosis surveillance area (DSA) in southwest Montana, USA. The monthly estimate was produced by summing estimates of the daily risk of abortion events during all days of the risk period. Note that portions of the counties that extend beyond the border of the DSA are not shown. Shading depicts hillshade of elevation.

**APPENDIX S8.** Monthly density of brucellosis-induced abortions from adult female elk.

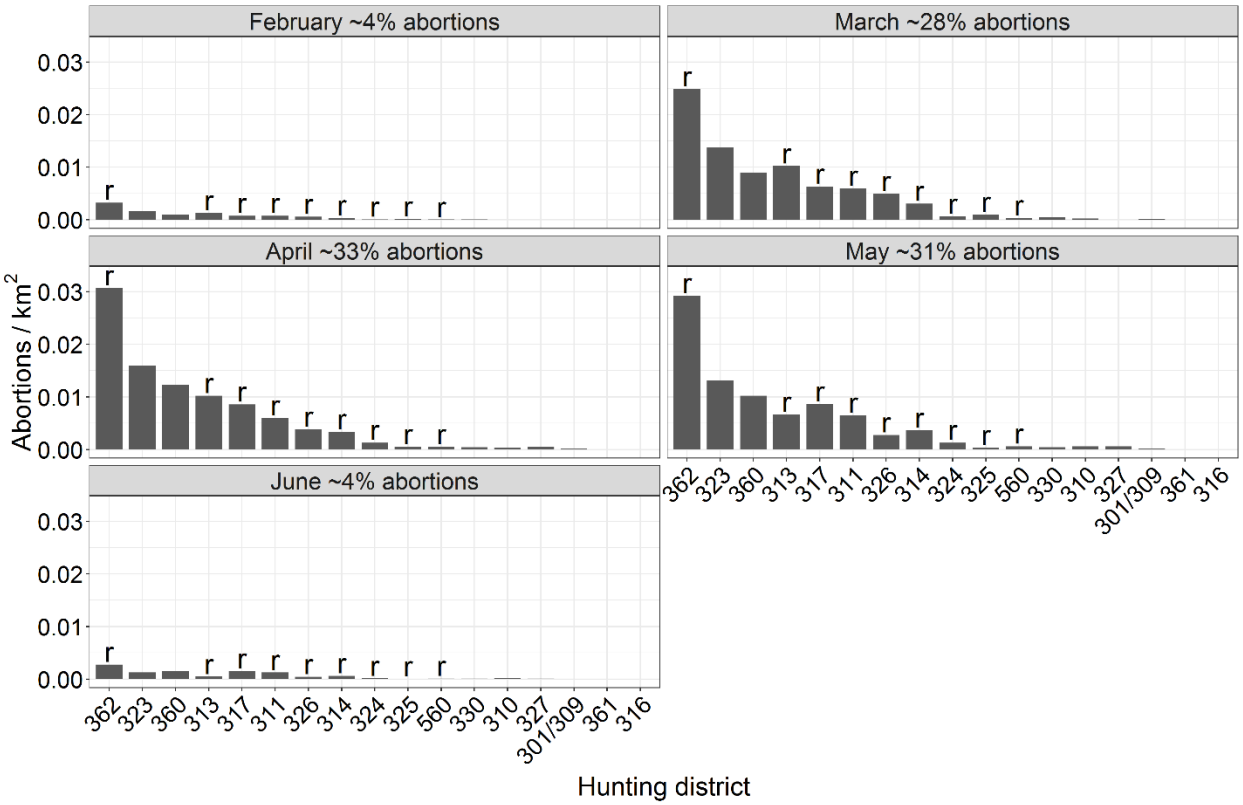


**Figure S1.** Monthly estimated density of brucellosis-induced abortions (abortions / $km^2$) from adult female elk on private ranchlands within the portion of elk hunting districts that fall within the boundary of the Montana designated brucellosis surveillance area (DSA) in southwest Montana, USA during the risk period (15 February-30 June) for brucellosis transmission. Percentages at the top of each panel indicate what percentage of the total risk period abortions on private grazing lands occurred during that month. Hunting districts where adult female elk were radiocollared are indicated by an 'r' at the top of the bars.